ARTICLE

Monoallelic *IFT140* pathogenic variants are an important cause of the autosomal dominant polycystic kidney-spectrum phenotype

Sarah R. Senum,[1] Ying (Sabrina) M. Li,[1,2] Katherine A. Benson,[3] Giancarlo Joli,[1,4] Eric Olinger,[5] Sravanthi Lavu,[1] Charles D. Madsen,[1] Adriana V. Gregory,[1] Ruxandra Neatu,[5] Timothy L. Kline,[6] Marie-Pierre Audrézet,[7] Patricia Outeda,[8] Cherie B. Nau,[9] Esther Meijer,[10] Hamad Ali,[11,12] Theodore I. Steinman,[13] Michal Mrug,[14,15] Paul J. Phelan,[16] Terry J. Watnick,[8] Dorien J.M. Peters,[17] Albert C.M. Ong,[18,19] Peter J. Conlon,[20] Ronald D. Perrone,[21] Emilie Cornec-Le Gall,[7] Marie C. Hogan,[1] Vicente E. Torres,[1] John A. Sayer,[5,22] Genomics England Research Consortium, the HALT PKD, CRISP, DIPAK, ADPKD Modifier, and TAME PKD studies, and Peter C. Harris[1,*]

Summary

Autosomal dominant polycystic kidney disease (ADPKD), characterized by progressive cyst formation/expansion, results in enlarged kidneys and often end stage kidney disease. ADPKD is genetically heterogeneous; *PKD1* and *PKD2* are the common loci (~78% and ~15% of families) and *GANAB*, *DNAJB11*, and *ALG9* are minor genes. PKD is a ciliary-associated disease, a ciliopathy, and many syndromic ciliopathies have a PKD phenotype. In a multi-cohort/-site collaboration, we screened ADPKD-diagnosed families that were naive to genetic testing (n = 834) or for whom no *PKD1* and *PKD2* pathogenic variants had been identified (n = 381) with a PKD targeted next-generation sequencing panel (tNGS; n = 1,186) or whole-exome sequencing (WES; n = 29). We identified monoallelic *IFT140* loss-of-function (LoF) variants in 12 multiplex families and 26 singletons (1.9% of naive families). IFT140 is a core component of the intraflagellar transport-complex A, responsible for retrograde ciliary trafficking and ciliary entry of membrane proteins; bi-allelic *IFT140* variants cause the syndromic ciliopathy, short-rib thoracic dysplasia (SRTD9). The distinctive monoallelic phenotype is mild PKD with large cysts, limited kidney insufficiency, and few liver cysts. Analyses of the cystic kidney disease probands of Genomics England 100K showed that 2.1% had *IFT140* LoF variants. Analysis of the UK Biobank cystic kidney disease group showed probands with *IFT140* LoF variants as the third most common group, after *PKD1* and *PKD2*. The proximity of *IFT140* to *PKD1* (~0.5 Mb) in 16p13.3 can cause diagnostic confusion, and *PKD1* variants could modify the IFT140 phenotype. Importantly, our studies link a ciliary structural protein to the ADPKD spectrum.

Introduction

Autosomal dominant polycystic kidney disease (ADPKD [MIM: 173900]) is the most common inherited kidney disease, occurring in ~1 in 1,000 individuals, and characterized by the progressive development and expansion of kidney cysts, leading to enlarged kidneys and often resulting in end stage kidney disease (ESKD).[1–3] Frequently found extrarenal manifestations include polycystic liver disease (PLD), which occasionally requires surgical intervention, and intracranial aneurysms that can rupture, causing subarachnoid hemorrhage.[4,5] Approximately 78% and 15% of cases have monoallelic pathogenic variants to *PKD1* (encoding polycystin 1, PC1, [MIM: 601313]) or *PKD2* (polycystin 2, PC2, [MIM: 173910]), respectively.[6,7] PKD1 is a more severe disease with an average age at ESKD of 58.0 years compared to 74.8 years for PKD2, and MRI-determined total kidney volume (TKV) strongly predicts disease severity.[8,9] PC1 and PC2 form a receptor complex, and a likely site for this complex associated with PKD is the primary cilium, a sensory antenna found on most cell types.[2,10]

[1]Division of Nephrology and Hypertension, Mayo Clinic, Rochester, MN 55905, USA; [2]Department of Nephrology, Chongqing Municipal Hospital of Traditional Chinese Medicine, Chongqing 400021, China; [3]School of Pharmacy and Biomolecular Science, Royal College of Surgeons in Ireland, Dublin 2, Ireland; [4]University Vita Salute San Raffaele, IRCCS San Raffaele Scientific Institute, 20132 Milan, Italy; [5]Translational and Clinical Research Institute, Faculty of Medical Sciences, Newcastle University, Newcastle upon Tyne, NE4 5PL, UK; [6]Department of Radiology, Mayo Clinic, Rochester, MN 55905, USA; [7]Univ Brest, Inserm, UMR 1078, GGB, CHU Brest, F-29200 Brest, France; [8]Division of Nephrology, University of Maryland School of Medicine, Baltimore, MD 21201, USA; [9]Department of Ophthalmology, Mayo Clinic, Rochester, MN 55905, USA; [10]Department of Nephrology, University Medical Center Groningen, University of Groningen, 9700 RB Groningen, the Netherlands; [11]Department of Medical Laboratory Sciences, Faculty of Allied Health Sciences, Health Sciences Center, Kuwait University, Sulaibikhat 90805, Kuwait; [12]Department of Genetics and Bioinformatics, Dasman Diabetes Institute (DDI), Dasman 15462, Kuwait; [13]Renal Division, Beth Israel Deaconess Medical Center, Boston, MA 02215, USA; [14]Division of Nephrology, University of Alabama, Birmingham, AL 35294, USA; [15]The Department of Veterans Affairs Medical Center, Birmingham, AL 35294, USA; [16]Renal Department, NHS Lothian - Royal Infirmary Edinburgh, Edinburgh, EH1 3EG, UK; [17]Department of Human Genetics, Leiden University Medical Center, 2300 RC Leiden, the Netherlands; [18]Kidney Genetics Group, Academic Nephrology Unit, Department of Infection, Immunity and Cardiovascular Disease, University of Sheffield Medical School, Sheffield, S10 2JF, UK; [19]The Sheffield Kidney Institute, Sheffield Teaching Hospitals NHS Foundation Trust, Sheffield, S10 2JF, UK; [20]Department of Nephrology, Beaumont Hospital and Department of Medicine Royal College of Surgeons in Ireland, Dublin 9, Ireland; [21]Division of Nephrology, Tufts Medical Center and Tufts University School of Medicine, Boston, MA 02111, USA; [22]Renal Services, Newcastle Upon Tyne Hospitals NHS Foundation Trust, and NIHR Newcastle Biomedical Research Centre, Newcastle University, Newcastle upon Tyne, NE4 5PL, UK
*Correspondence: harris.peter@mayo.edu
https://doi.org/10.1016/j.ajhg.2021.11.016.

The application of next-generation sequencing (NGS), including whole-exome sequencing (WES) and panels targeting a more limited number of genes (tNGS), to individuals with ADPKD-like phenotypes has identified new loci, including *GANAB* (MIM: 104160), *DNAJB11* (MIM: 611341), and *ALG9* (MIM: 606941), partially accounting for the ~7% of non-PKD1 or -PKD2 families.[11–13] *GANAB* is rarely associated with ESKD and can also cause autosomal dominant PLD (ADPLD), an ADPKD-related disorder but with few kidney cysts.[11,14] *GANAB* encodes glucosidase IIa (GIIa); pathogenic variation in its binding partner GIIb (encoded by *PRKCSH* [MIM: 177060]) is a common cause of ADPLD.[15,16] In contrast, DNAJB11-nephropathy is characterized by the development of small kidney cysts and fibrosis and resulting in ESKD in later life,[12,17] a phenotype related to autosomal dominant tubulointerstitial kidney disease (ADTKD [MIM: 162000]) due to *UMOD* (MIM: 162000) or *MUC1* (MIM: 158340) pathogenic variants.[18] The ALG9 phenotype is of moderate cystic kidney disease and occasional ESKD.[13] *DNAJB11* encodes the endoplasmic reticulum (ER) protein ERdj3, a co-factor of the chaperone protein BiP, while *ALG9* encodes the ALG9 alpha-1,2-mannosyltransferase. These three gene products are involved in the glycosylation, folding, quality control, and trafficking of membrane and secreted proteins in the ER.[19] Processing of the large, glycosylated membrane protein, PC1, is particularly inhibited by loss or reduction of these ER proteostasis proteins.[11–14] There is also phenotypic overlap between the ADPKD spectrum and ADTKD-*HNF1B* (MIM: 189907) and several other monogenic disorders.[20–24] Together these minor loci account for some but not all non-PKD1 or -PKD2 ADPKD-like subjects.

Autosomal recessive PKD (ARPKD) is caused by bi-allelic pathogenic variants in *PKHD1* (encoding fibrocystin, FPC [MIM: 606702]), and the typical phenotype is large echogenic kidneys detected *in utero* or during infancy with significant neonatal lethality and childhood ESKD, although milder, later childhood or even adult-onset disease can occur.[2] In ARPKD, the liver phenotype is mainly congenital hepatic fibrosis rather than PLD, and single *PKHD1* pathogenic variants have been associated with mild cystic kidney and/or cystic livers.[14,25] FPC has also been associated with cilia. In addition to these simple kidney- and liver-focused disorders, a wide range of syndromic diseases associated with cilia, ciliopathies, have kidney and liver phenotypes, including the bi-allelic Meckel syndrome (MKS [MIM: 249000]), Senior-Loken syndrome (SLS [MIM: 266900]), Joubert syndrome (JBTS [MIM: 213300]), short-rib thoracic dysplasia (SRTD [MIM: 208500]), and Bardet-Biedl syndrome (BBS [MIM: 209900]), and the X-linked dominant orofaciodigital syndrome type 1 (OFD1 [MIM: 311200]).[26–28] The kidney and liver phenotypes include cysts, nephronophthisis (NPHP [MIM: 256100]; tubulointerstitial nephritis and renal fibrosis without kidney enlargement), and congenital hepatic fibrosis. Reflecting the signaling and transporting roles of cilia during development and later, a wide range of additional phenotypes are found in these syndromic ciliopathies. Organ involvement includes the central nervous system, ranging from encephalocele (MKS), through hypoplasia of the cerebellar vermis (JBTS), to developmental delay (BBS); eye, retinal degeneration manifesting as retinitis pigmentosa or Leber congenital amaurosis (SLS, JBTS, SRTD, BBS); bone, including abdominal skeletal disorders (SRTD), craniofacial abnormalities (SRTD), and polydactyly (MKS, JBTS, SRTD, BBS); and obesity (BBS). Rare variants in at least 70 genes cause syndromic ciliopathies with kidney involvement, and most encode proteins involved in determining ciliary structure and/or function.[29] These range from proteins involved in intraflagellar transport (IFT), anterograde and retrograde transport systems required to generate the cilium, transport proteins along its length, and for appropriate signaling; transition zone proteins that form a barrier regulating the protein composition of the cilium; and cargo adaptor proteins.[28,30,31] The cystic kidney disease associated with these syndromic PKD ciliopathies may be due to reduced polycystin-complex (and/or FPC) in the cilium,[32–34] analogous to the ER proteostasis defects causing ADPKD/ADPLD. However, the finding from *in vivo* studies that cilia removal in the kidney in the context of PC1 loss partially rescues PC1-associated cystic disease questions whether there are additional ciliary factors causing or preventing PKD.[10,35]

Here, employing NGS of ADPKD-like individuals and analysis of large, sequenced populations, we provide evidence that monoallelic pathogenic variants to a cilia component gene are an important cause of the ADPKD phenotype.

Subjects and methods

Study participants and clinical analysis

Details of the study participants and their recruitment sites are summarized in Figure 1. Subjects were recruited from ADPKD clinical trials: HALT-PKD (n = 49),[36,37] TAME-PKD (n = 83),[38] and DIPAK (n = 12);[39] observational ADPKD studies: Consortium for Radiologic Imaging Studies of Polycystic Kidney Disease (CRISP) (n = 11),[40] Genkyst (n = 10),[41] and DIPAK Observational Study (n = 137);[42] genetic studies of ADPKD: ADKPD Modifier Study (n = 49), the Mayo PKD Center (n = 737), and the Irish Kidney Gene Project (IKGP; n = 35);[43] and from other academic centers studying ADPKD. The relevant institutional review boards or ethics committees approved all studies, and participants gave informed consent. Clinical and imaging data were obtained by review of clinical records. Hypertension was recorded as the age at which the individual started anti-hypertensive medications or had two or more consecutive readings of 140/90 or above. Kidney volumes were measured by stereology or automatedly[44] from the most recent abdominal CT or MRI and the Mayo Imaging Class (MIC) was determined.[8] Kidney function was calculated as estimated glomerular filtration rate (eGFR; mL/min/1.73 m^2) from clinical serum creatinine measurements with the Chronic Kidney Disease Epidemiology Collaboration (CKD-EPI) formula.[45] Blood or buccal samples for standard DNA isolation were collected from the probands and all available family members.

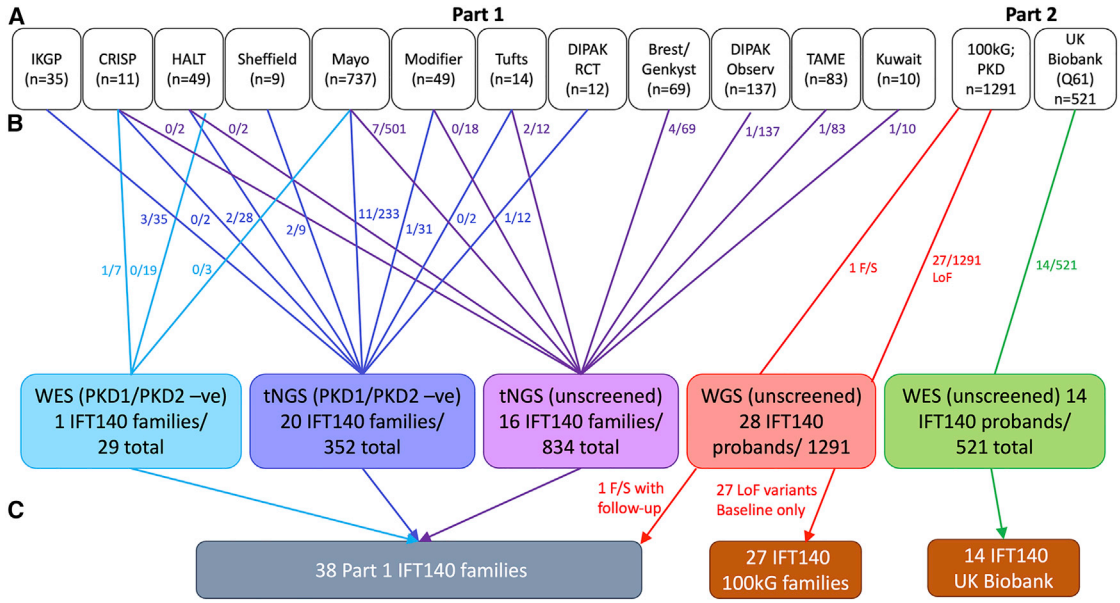

Figure 1. Details of the study design

(A) The study is divided into screening of ADPKD spectrum families (part 1) and analysis of previously sequenced cohorts (part 2). Part 1 included subjects from ADPKD clinical trials: HALT PKD (HALT), DIPAK randomized clinical trial (RCT), and TAME; ADPKD observational studies: CRISP, DIPAC Observational (Observ), and Genkyst; genetics studies: ADPKD Modifier, Mayo PKD Center, and Irish Kidney Gene Project (IKGP); and other recruitment sites: Sheffield, Tufts, Brest, and Kuwait. Part 2 consisted of the Genomics England 100K project Cystic Kidney Disease cohort (100kG; PKD) and the UK Biobank (individuals with ICD-10 Q61). The number of analyzed individuals per study site is indicated.

(B) The sequencing methods and whether participants were prescreened for *PKD1* and *PKD2* are indicated, the total number of screened and IFT140-positive families is shown. The number of families/probands with pathogenic *IFT140* variants relative to the total number screened by each method from each study/site are shown above. Out of the 777 naive families screened at Mayo, 357 (45.9%) and 105 (13.5%) were resolved by pathogenic or likely pathogenic *PKD1* or *PKD2* variants, respectively, while 30 (3.9%) and six (0.8%) had a VUS to *PKD1* or *PKD2*. Among the pathogenic variants were 19 *PKD1* large deletions, one *PKD1* large duplication, and three *PKD2* large deletions. The relatively low number of families resolved with a *PKD1* or *PKD2* pathogenic variant (59.5%), reflects the broad phenotypic spectrum of the recruited individuals, including mild cystogenesis.

(C) Summary of the screening showing the total number of IFT140 families identified by screening of ADPKD spectrum subjects (part 1) and identified in the 100kG, PKD cohort, and the UK Biobank (part 2).

Targeted next-generation sequencing (tNGS)

Screening was performed using either a 137 or 357 gene tNGS panel containing known and candidate PKD and ciliopathy genes,[38,46] and for the 35 IKGP and 69 Brest/Genkyst individuals, as described, respectively, with *IFT140* added to the French panel.[17,43] As indicated in Figure 1, causative variants in *PKD1* or *PKD2* were not found in previous testing of 352 families, while 834 families had not been previously screened. Library preparation, sequencing, read-alignment, and variant calling were performed as previously described.[12,46] Variant mining was performed with SNP and Variation Suite (v.8.9.0, Golden Helix; SVS) after employing the following filters: (1) variant-based read depth (DP $\geq$ 10×) and genotype quality (GQ $\geq$ 20), (2) removal of variants with minor allele frequency (MAF) $>$ 0.01 in gnomAD, and (3) removal of variants $>$ 40 bp from target coding regions.

Whole-exome sequencing (WES)

Twenty-nine previously unresolved families were screened by WES at the Mayo Clinic. Genomic DNA (500 ng) was sheared by ultrasonication, and libraries were prepared on an Agilent Bravo system with the NEBNext UltraDNA Preparation Kit. Samples were pooled in groups of 12 prior to capture with the Agilent SureSelectXT Human All Exon V7 kit. Samples were sequenced by the Mayo Clinic Genome Analysis Core with 150 bp paired-end reads on an Illumina HiSeq4000 with one pool per lane. Read alignment and variant calling was performed with the same methodology as the tNGS panels. Variant mining was done in SVS with the following filters: (1) variant DP $\geq$ 5× and GQ $\geq$ 10, (2) removal of variants with MAF $>$ 0.001 in gnomAD, and (3) removal of variants $>$ 40 bp from coding regions.

Sanger screening, copy number variant analysis, and variant assessment and confirmation

In samples where no causative variant was identified, *PKD1* and *PKD2* were further screened via exon-specific amplification and Sanger sequencing, with the duplicated region of *PKD1* first amplified by previously described long-range PCR.[46] Large copy number variants (CNVs) were assessed from the NGS by calculating the log2 ratio of actual read-depth over the expected read-depth for a given locus, and suspected variants confirmed by multiplex ligation-dependent probe amplification (MLPA).[46] Exon specific PCR primers were designed for confirmation of variants identified in *IFT140* (Table S1) and other genes of interest. Variants of interest in probands and any available family members were confirmed and segregated by amplifying 100 ng of gDNA and Sanger sequenced bi-directionally at GeneWiz. We analyzed Ab1 files by employing Mutation Surveyor (V5.1.1, SoftGenetics) to confirm the variant.

The possible significance of missense changes was assessed with the tools SIFT, PolyPhen-2, MutationTaster, MutationAssessor, PROVEAN, FATHMM, and CADD and more broadly as previously described.[6,12,43] The pathogenicity of variants was assessed by the American College of Medical Genetic (ACMG) guidelines.[47] Splicing evaluation was performed with the Berkeley *Drosophila* Genome Project (BDGP) Splice Site Prediction by Neural Network and Genomnis Human Splice Finder (HSF) sites.[48,49] Where possible, the phase of *IFT140* and *PKD1* variants was determined by segregation analysis in families.

Genomics England 100K project

All participants in the 100K Genomes Project (100kG) provided written consent to access their anonymized clinical and genomic data for research purposes. The project model and its informed consent process have been approved by the National Research Ethics Service, Research Ethics Committee for East of England (Cambridge South Research Ethics Committee). Whole-genome sequencing (WGS) was performed with the Illumina TruSeq DNA PCR-Free sample preparation kit (Illumina) and an Illumina HiSeq 2500 sequencer, generating a mean depth of 45× (range from 34× to 72×) and greater than 15× for at least 95% of the reference human genome. WGS reads were aligned to the Genome Reference Consortium human genome build 37 (GRCh37) with Isaac Genome Alignment Software (version 01.14; Illumina). Sequence data were analyzed with bcftools scripts designed to search vcf.gz files, and individual BAM files were viewed with IGV. Variant annotation was performed with Ensembl Variant Effect Predictor (VEP) with the following filter: canonical transcript (ENST00000426508.7) *IFT140* gene and high impact (see results for details). Phenotypes of identified carriers were manually reviewed in Genomics England Participant Explorer. We reviewed exit questionnaires, filled in by the clinicians at the NHS Genomics Medical Centres (GMCs) for each closed case, to detect subjects solved for other genes. Those recruited under the "normalized specific disease" term cystic kidney disease, included 1,550 individuals from 1,291 families.

UK Biobank

UK Biobank is a large prospective study with over 500,000 participants aged 40–69 years when recruited in 2006–2010 and globally accessible to approved researchers who are undertaking health-related research that's in the public interest.[50] Exome data on ~200,000 individuals have been made available.[51] Ethics approval for the UK Biobank study was obtained from the North West Centre for Research Ethics Committee (11/NW/0382). The exome data of 200,643 individuals were accessed for variants in *IFT140* (GRCh38: chr16: 1,510,427–1,612,072) and filtered with Ensembl VEP for high or rare (gnomAD_AF $\leq$ 0.1%), low impact alleles (see results for details) predicted for the canonical transcript ENST00000426508.7. IMPACT predictions were a subjective classification of the severity of the variant consequence based on agreement with SNPEff (see also results). UK Biobank diagnoses and disease terms recorded in carriers of high and low impact variants were extracted, manually reviewed, and filtered for ICD-10 classifiers of kidney disease: Q61.x (cystic kidney disease), N28.1 (cyst of kidney), N18.x (chronic kidney disease), N17.x (acute renal failure), I12.x (hypertensive renal disease), and N20.0 (calculus of kidney); the term x indicates that all sub-classifications were taken into consideration (e.g., N18.x includes all stages of CKD corresponding to N18.1–N18.5 and N18.9 for unspecified CKD). A Fisher's exact two-sided test was used for enrichment of diagnoses in high impact variant carriers, and $p \leq 0.05$ was considered statistically significant.

The AstraZeneca PheWAS Portal is a repository of gene-phenotype associations for data derived from electronic health records, questionnaires, and continuous traits computed on exomes released by UK Biobank. Gene-level associations were tested with collapsing analyses comparing the proportion of cases with a qualifying variant with the proportion of controls with a qualifying variant in each gene. Twelve different sets of qualifying variant filters (models: ten dominant models, one recessive model, and one synonymous variant model) were applied to test the association between 18,762 genes and 18,780 phenotypes after extensive quality control filters.[52] Here, we analyzed the gene associations with cystic kidney disease (ICD-10 code Q61) by using the collapsing model Ptv5pcnt (protein-truncating variants; PTVs, MAF $\leq$ 5% both within the cohort and gnomAD). PTVs were designated based on SnpEff annotations and defined as frameshifting, nonsense, typical splicing, copy number variant, and rare missense. Collapsing analysis p values were generated with a Fisher's exact two-sided test. A study-wide significance threshold of $p \leq 2e^{-9}$ was defined on the basis of an empirical null distribution with the synonymous collapsing model and an n-of-1 permutation-based null distribution.

Results

Study design

The design of this multinational collaborative study to identify genes harboring variants causative of an ADPKD-like phenotype is shown in Figure 1. Part 1 included screening individuals diagnosed with ADPKD or cystic kidneys, with the vast majority meeting the imaging criteria for ADPKD,[53,54] by tNGS (n = 1,186) or WES (n = 29). Recruitment occurred from 12 different sites or studies and includes subjects for whom previous *PKD1* and *PKD2* sequencing did not identify a causative variant (n = 381) and unscreened populations (n = 834), with a total of 1,215 families screened (see Figure 1 for details). Part 2 of the study included analysis of large populations of individuals that were genetically characterized by WGS, the cystic kidney disease cohort from Genomics England 100K project (100kG; PKD), or WES, the UK Biobank ICD 10 code, Q61: cystic kidney disease (UK Biobank; Q61; Figure 1). One family detected in the 100kG (PKD) project where follow up was possible was analyzed in part 1 of the project.

IFT140 is an ADPKD-spectrum candidate gene

A gene with loss-of-function (LoF) variants identified in multiple ADPKD families from the tNGS analysis in part 1 of the study was *IFT140* (MIM: 614620; Chr. 16p13.3). *IFT140* has 29 exons and a coding region of 4,386 bp (GenBank: NM_014714.4) and encodes the IFT140 protein of 1462aa (GenBank: NP_055529.2). IFT140, is a principal component of the IFT-A core complex (along with IFT122 and WDR19 [IFT144]), while IFT43, WDR35 (IFT121), and TTC21B (IFT139) form a peripheral subcomplex.[55] The IFT-A proteins are responsible for dynein-associated retrograde

trafficking of proteins from the ciliary tip back to the basal cell body.[33,55–57] *IFT140* bi-allelic pathogenic variants have been associated with the syndromic ciliopathy SRTD (SRTD9 [MIM: 266920]), also described as Jeune asphyxiating thoracic dystrophy or Sensenbrenner or Mainzer-Saldino syndromes.[58–60] The SRTD9 phenotype includes retinal dystrophy, skeletal malformations (including small thorax, cone-shaped epiphyses, craniofacial abnormalities, and digit malformations), and chronic kidney disease (cysts and fibrosis).[58,59] In addition, bi-allelic variants to *IFT140* are associated with non-syndromic forms of retinal dystrophy (MIM: 617781), Leber congenital amaurosis, and retinitis pigmentosa.[61,62] Conditional knockout of *Ift140* in mouse kidney collecting ducts (HoxB7-Cre) demonstrated extensive cystic growth and fibrosis by P20 and short, stumpy cilia.[63] Therefore, *IFT140* was a strong candidate as an ADPKD phenotype gene.

Families with monoallelic *IFT140*-truncating variants

To determine whether *IFT140* variants are causing cystic disease in a monogenic fashion, it was important to demonstrate segregation in families. From our screening, 12 multiplex families with two or more members with *IFT140* pathogenic variants and a cystic kidney phenotype were identified, and there was a total of 40 affected individuals. Clinical details of these families are summarized in Tables 1 and S2 and details of the pathogenic *IFT140* variants are shown in Table 2.

Pedigree M132

In family M132, PKD was diagnosed in four generations, and no pathogenic *PKD1* or *PKD2* variants were identified from Sanger analysis in the family (Figure 2A). The canonical *IFT140* splicing variant c.2399+1G>T was identified simultaneously in an uncle (II-3) and nephew (III-1) by tNGS. Subsequently, the variant was confirmed in III-2, and II-2 was an obligate carrier. A distinctive phenotype of a few, large bilateral kidney cysts but without liver cysts were seen in II-3, III-1, and III-2 (Figures 2B–2D), and reduced eGFR was seen in III-1. A mild cystic phenotype was also seen in II-1 and IV-1 (Figures 2E and 2F), and enlarged cystic kidneys described in the grandfather (I-2), but DNA was not available. Of the seven known and presumed affected members, none experienced ESKD.

Pedigree M199

PKD was diagnosed in seven individuals over two generations in M199 (Figure 2G). Screening by tNGS identified the *IFT140* frameshifting variant c.2767_2768+2del (p.Tyr923fs*18) in the four affected members with DNA available. Kidney imaging was available for five individuals, and the disease was characterized by a few, larger cysts and in some cases asymmetry between the kidneys, with a single large cyst particularly prominent in III-2 (Figures 2H–2K and S1A–S1C). Four members had renal insufficiency in their 70s, including II-2 with type 2 diabetes, who was approaching ESKD when he died at 72 years old.

Pedigree P1320

The proband, II-1, was diagnosed at 66 years with abdominal pain, and ultrasound revealed mild, bilateral kidney cysts and a single liver cyst (Figures 2L and 2M). Follow up ultrasound and MRI determined that two of her four children had kidney cysts (Figure 2N), as well one of her sisters (II-2). Screening II-2 by tNGS identified the frameshift variant, *IFT140*: c.2285_2286del (p.Phe762fs*39), which was confirmed in the three other affected subjects.

Pedigree EDI1005

The three living affected members of this family were screened by WGS as part of the 100kG Project (but where follow-up clinical and imaging analysis was possible) and all were found to have the *IFT140* frameshifting variant, c.992_993del (p.Cys331fs*3) (Figure 2O). Follow-up imaging analysis revealed large kidneys due to just a few large bilateral cysts, and some kidney asymmetry was seen in each individual (Figures 2P–2R). The father (I-1) was diagnosed with kidney cysts at 80 years old and died at 89 years old without ESKD.

Pedigree 390044

The HALT study proband (III-1) was diagnosed at 41 years old with a few bilateral kidney cysts, including exophytic cysts (Figures 2S and 2T). Her mother (II-2) had mild cystic disease, while an aunt (II-1) with PKD had a right kidney nephrectomy at 66 years old (Figures 2U and 2V). Genetic analysis of III-1 and II-2 identified the *IFT140* frameshifting variant c.2483delG (p.Gly828fs*18) (DNA was not available from II-1). There was no known prior family history, but the grandparents died in their 50s with limited clinical information available.

Pedigree M1629

The proband, III-2, had multiple bilateral cysts and normal renal function, her father (II-1) had large cysts in both kidneys and declining renal function, and her brother (III-1) mild PKD and normal kidney function (Figures 3A–3C and S1D). The typical splicing change, *IFT140*: c.2400−2A>T, was identified or inferred from a linked *PKD1* variant.

Pedigree PK14083

Two siblings (II-1 and II-2) had large, bilateral kidneys cysts without liver cysts, and their mother was diagnosed with PKD but died at 92 years old without ESKD (Figures 3D–3F). Both siblings had the *IFT140* frameshift variant c.3696delG (p.Ile1234fs*33).

Pedigree M1554

The mother (II-1) had asymmetric disease with two large left kidney cysts, while the daughter (III-1) has almost unilateral disease with multiple right kidney cysts (Figures 3G–3I). Both had normal kidney function and shared the *IFT140* frameshifting variant c.2767_2768+2del.

Pedigree P1497

In this family from the DIPAK randomized clinical trial (RCT), two sisters shared the *IFT140* frameshift variant c.1655_1656del (p.Glu552fs*6); II-1 had multiple large cysts with some asymmetry, and II-2 had just a few cysts

Table 1. Details of individuals with *IFT140* pathogenic variants

Demographics			Clinical details			Kidney imaging								
								Cyst	Volume (mL/m) or length (cm)					
Pedigree (study)	Subject	Sex	Dx age	eGFR, age	HTN, age	Type	Age	description	htRK	htLK	htTKV	MIC	Figure	Liver cysts
Families														
M132 (Mayo)	I-2[a]	female	N/A	N/A	yes, ?	N/A	–	MLg, RKN	–	–	–	–	–	N/A
	II-1[a]	male	N/A	43, 94 y	yes, ?	CT	91 y	BMLg, LKEx	221	427	648	2A	Figure 2E	N/A
	II-2[b]	male	N/A	46, 72 y	yes, ?	N/A	–	BLg	–	–	–	–	–	N/A
	II-3	male	69 y	66, 74 y	no, ?	MRI	69 y	BMLg, LKEx	360	566	926	1B	Figure 2B	none
	III-1	male	54 y	47, 66 y	no, ?	MRI	63 y	BM	393	436	830	1B	Figure 2C	none
	III-2	male	40 y	109, 47 y	no, ?	MRI	45 y	BCl	425	197	622	2A	Figure 2D	none
	IV-1[a]	female	38 y	81, 38 y	no, 39 y	CT	38 y	RKFLg, LKDP	89	79	169	2A	Figure 2F	2S
M199 (Mayo)	II-1	female	59 y	57, 87 y	yes, <72 y	CT	81 y	BFEx	–	–	–	2A	Figure 2H	N/A
	II-2[a]	male	N/A	21, 70 y	N/A	N/A	–	–	–	–	–	–	–	N/A
	II-3[a]	male	77 y	41, 78 y	yes, <75 y	CT	77 y	BMEx	308	454	762	1B	Figure 2I	none
	II-4	male	74 y	35, 74 y	yes, <42 y	US	74 y	BLg	–	–	–	–	Figures S1A and S1B	none
	III-1	female	39 y	55, 73 y	no, 74 y	MRI	57 y	BLgEx	166	106	272	2A	Figure 2J	none
	III-2	female	58 y	87, 71 y	yes, 63 y	CT	58 y	BF, LK1Lg	10.9 c	13.6 c	–	2A	Figure 2K	none
	III-4	male	–	38, 72 y	yes, <68 y	CT	69 y	BFCl	170	131	301	2A	Figure S1C	none
P1320 (Shef)	II-1	female	69 y	46, 77 y	yes, ?	MRI	69 y	BMLg	17.9 c	15.4 c	–	–	Figure 2M	1
	II-2	female	66 y	73, 69 y	yes, ?	US	66 y	BFLg	13 c	13 c	–	–	–	none
	III-2	female	46 y	58, 52 y	N/A	MRI	46 y	LK1 RK5	10.7 c	13.2 c	–	2A	Figure 2N	none
	III-4	male	40 y	94, 43 y	N/A	US	40 y	BMLg	12.4 c	12.9 c	–	–	–	none
EDI1005 (100kG)	I-1[a]	male	80 y	N/A	N/A	autopsy	89 y	BLg	–	–	–	–	–	N/A
	II-1	female	N/A	56, 68 y	yes, ?	CT	58 y	BMLg	1,340	966	2,306	1D	Figure 2P	FS
	III-1	male	33 y	99, 37 y	no, 37 y	MRI	33 y	BMLg	540	262	802	1D	Figure 2Q	none
	III-2	female	30 y	85, 39 y	no, 39 y	US	37 y	BMLg	–	–	–	–	Figure 2R	none
390044 (HALT)	II-1[a]	female	–	59, 86 y	yes, 66 y	CT	86 y	MLg, RKN	N	253	–	–	Figure 2V	none
	II-2	female	63 y	51, 79 y	yes, <65 y	CT	63 y	FLg, LKN	–	–	–	–	Figure 2U	F
	III-1	female	41 y	45, 58 y	yes, 37 y	CT	58 y	BMEx	348	864	1,212	1C	Figure 2T	none
M1629 (Mayo)	II-1	male	71 y	39, 73 y	yes, <61 y	MRI	71 y	BMLg&S	450	517	967	1B	Figure 3C	FS
	III-1	male	40 y	80, 40 y	yes, <40 y	US	40 y	BFLg	11.1 c	11.2 c	–	–	Figure S1D	none
	III-2	female	39 y	107, 40 y	no, 40 y	CT	39 y	BF	137	134	272	1B	Figure 3B	FS
PK14083 (Brest)	II-1	male	62 y	57, 65 y	yes, 55 y	MRI	62 y	BLgEx	333	508	841	2A	Figure 3E	none
	II-2	female	58 y	37, 63 y	yes, 55 y	MRI	62 y	MBLg	177	221	398	2A	Figure 3F	none
M1554 (Tufts)	II-1	female	53 y	82, 57 y	yes, <53 y	CT	53 y	A LKFLg	10.5 c	18.8 c	–	2A	Figure 3H	none
	III-1	female	34 y	84, 36 y	no, 36 y	CT	34 y	U RKMLg	–	–	–	2A	Figure 3I	none
P1497 (DIPAK^{R})	II-1	female	51 y	85, 56 y	yes, 51 y	MRI	57 y	A LKMLg	773	329	1,102	2A	Figure 3K	none
	II-2	female	39 y	83, 54 y	no, 54 y	MRI	54 y	A LKM RKFS	114	219	333	2A	Figure 3L	none
1470059 (Mod)	II-1	male	72 y	44, 79 y	yes, 54 y	MRI	76 y	BMLgEx	822	952	1,774	1C	Figure 3N	none
	III-1	male	45 y	84, 49 y	no, 49 y	MRI	49 y	BFSEx	114	159	273	1A	Figure 3O	none

(*Continued on next page*)

Table 1. *Continued*

Demographics			Clinical details			Kidney imaging								
								Cyst	Volume (mL/m) or length (cm)					
Pedigree (study)	Subject	Sex	Dx age	eGFR, age	HTN, age	Type	Age	description	htRK	htLK	htTKV	MIC	Figure	Liver cysts
M1169 (Mayo)	I-1	male	–	50, 84 y	yes, 81 y	US	?	2 LK	–	–	–	–	–	N/A
	II-1	female	46 y	102, 50 y	no, 50 y	CT	46 y	BF	141	163	304	1B	Figure 3Q	none
M1266 (Mayo)	II-1	female	–	65, 67 y	no, 67 y	US	66 y	BM FLg	9.6 c	9.3 c	–	–	–	none
	II-2	female	45 y	80, 58 y	no, 59 y	MRI	55 y	FS	67	69	136	1A	Figure 3S	MnS
Singletons														
440003 (CRISP)	406737	female	41 y	74, 54 y	no, 54 y	MRI	53 y	BF	199	107	307	1A	Figure S2A	none
690036 (HALT)	E4669644	male	51 y	38, 68 y	yes, 51 y	US	58 y	BM	–	–	–	–	–	–
F430 (Dublin)	8143	male	31 y	67, 45 y	no, 46 y	US	31 y	BF	12.6 c	12 c	–	–	–	none
F392 (Dublin)	10235	female	45 y	94, 58 y	yes, 50 y	US	45 y	BMLg	9.7 c	10.7 c	–	2A	Figure S1E	none
F662 (Dublin)	10664	female	N/A	69, 76 y	yes, 58 y	US	70 y	A RK2Lg, LKMLg	14.8 c	11.2 c	–	–	Figure S1F	none
M120 (Mayo)	R1097	female	46 y	70, 65 y	yes, 45 y	MRI	65 y	BMEx RK1Lg	296	222	519	2A	Figure S3F	none
M154 (Mayo)	R1142	female	57 y	68, 64 y	yes, <50 y	CT	64 y	A BMLg	451	946	1,397	2A	Figure S2B	none
M187 (Mayo)	R19	female	53 y	35, 79 y	yes, 53 y	CT	78 y	BMLg	1,025	994	2,019	1C	Figure S2C	none
M241 (Mayo)	R1403	male	74 y	30, 85 y	yes, <69 y	CT	83 y	BMLg	498	562	1,060	1A	Figure S2D	none
M274 (Mayo)	R1367	female	72 y	43, 90 y	yes, <72 y	MRI	79 y	A LKFLg, RKS	81	375	455	2A	Figure S2E	none
M323 (Mayo)	R1606	male	58 y	41, 67 y	yes, <68 y	US	67 y	BMLg	–	–	–	–	–	none
M357 (Mayo)	R874	female	50 y	49, 76 y	yes, <62 y	CT	76 y	A LKFL, RKM	1,325	471	1,796	2A	Figure S2F	none
M614 (Mayo)	R1942	male	46 y	82, 59 y	yes, 45 y	CT	53 y	BFLgEx	353	253	606	2A	Figure S2G	none
M1062 (Mayo)	R2939	male	56 y	52, 62 y	yes, 55 y	CT	62 y	A RK <5Lg, LK 1Lg	776	359	1,135	2A	Figure S2H	none
M1111 (Mayo)	R2995	male	50 y	46, 55 y	no, 52 y	MRI	52 y	BFS	101	122	222	1A	Figure S2I	none
M1261 (Tufts)	R3221	female	29 y	99, 34 y	no, 32 y	CT	30 y	FS RK1Lg	217	158	375	2A	Figure S2J	none
M1277 (Mayo)	R3248	male	56 y	ESKD, 64 y	yes, 56 y	CT	61 y	RKN WT6m, LKMEx	N	261	–	–	Figure S3A	FS
M1374 (Mayo)	R3376	female	65 y	62, 68 y	yes, 67 y	CT	68 y	BFLK1Lg	927	562	1,489	2A	Figure S2K	none
M1540 (Mayo)	R2098	male	64 y	57, 65 y	yes, <65 y	CT	66 y	BFEx	152	315	468	1B	Figure S3D	none
P1195 (Shef)	Ox3922	female	57 y	50, 92 y	yes, ?	CT	92 y	BMLgEx	17 c	23 c	–	–	Figure S2L	none
P1480 (Kuw)	Ox5181	female	44 y	130, 44 y	yes, 40 y	US	44 y	LK8 RK8	456	420	876	1C	–	none
P1504 (DIPAK^{O})	Ox5058	male	52 y	43, 57 y	yes, 48 y	MRI	61 y	MBLg	1,371	1,376	2,747	1D	Figure S2M	M
P1505 (TAME)	Ox5262	female	50 y	70, 52 y	yes, 41 y	MRI	52 y	A LK2Lg RK FS	179	709	888	2A	Figure S2N	none
PK14084 (Genkyst)	210192	female	37 y	105, 48 y	no, 48 y	MRI	48 y	FBLg	218	158	376	2A	Figure S3H	none
PK14082 (Brest)	200138	female	44 y	77, 44 y	no, 44 y	CT	44 y	FBLg	109	170	270	2A	Figure S2O	none
PK14085 (Brest)	210193	female	75 y	57, 75 y	no, 75 y	CT	75 y	FBLg	142	106	248	2A	Figure S2P	none

DIPAK^{R}, DIPAK randomized clinical trial; 100kG, 100,000 Genomes; Kuw, Kuwait; Mod, Modifiers of ADPKD Study; Shef, Sheffield; DIPAK^{O}, DIPAK observational study; Dx age, age at diagnosis; HTN, hypertension; N/A, not available; y, years; ?; unknown; A, asymmetric presentation; B, bilateral; Cl, clustered; DP, dilated pelvis; Ex, some exophytic; F, few; LK, left kidney; Lg, large; M, multiple; Mn, many; N, nephrectomy; RK, right kidney; S, small; U, unilateral; WT, Wilms tumor; htRK, height-adjusted right kidney volume; htLK, height-adjusted left kidney volume; htTKV, height-adjusted total kidney volume.
[a]No sample for genetic confirmation.
[b]Genotype inferred.

Table 2. Details of the *IFT140* pathogenic variants

cDNA variant[a]	Protein variant	Type	Effect	GnomAD v2.1.1	Publication	ClinVar	ACMG designation	Part 1 pedigrees	100,000 Genomes pedigrees
c.223delG	p.Val75fs*11	FS del	truncating	0	–	N	LP	M1266	–
c.490G>T	p.Glu164*	nonsense	truncating	0	Schmidts et al.[59]	N	P	F392, M614, M1261	–
c.581delT	p.Leu194fs*2	FS del	truncating	0	–	N	LP	440003	–
c.594dupG	p.Ser199fs*21	FS dup	truncating	0	–	N	LP	M1374	–
c.634G>A	p.Gly212?	splice	non trunc	15/282, 764	Perrault et al.[58]	8× P, 2× LP	LP	M1277	–
c.810+1G>A	p.Lys270?	splice	truncating	0	–	N	LP	–	UK25
c.931dupT	p.Tyr311fs*7	FS dup	truncating	0	–	N	LP	690036	–
c.992_993del	p.Cys331fs*3	FS del	truncating	0	–	N	LP	EDI1005	–
c.1010−1G>A	p.Gly337?	splice	truncating	11/279,352	–	5× P	P	F662, PK14082	–
c.1039C>T	p.Arg347*	nonsense	truncating	1/250,764	–	N	LP	–	UK11
c.1147C>T	p.Gln383*	nonsense	truncating	1/31,360	–	N	LP	–	UK4
c.1246C>T	p.Gln416*	nonsense	truncating	6/249,758	–	N	LP	–	UK10, UK17
c.1359+1G>A	p.Lys453?	splice	truncating	0	–	1× LP	LP	–	UK16
c.1377G>A	p.Trp459*	nonsense	truncating	22/215, 228	Xu et al.[62]	1× P	P	M241, M274, M1169, P1505	UK12, UK14, UK26
c.1525−1G>A	p.Gly509?	splice	truncating	0	–	1× LP	LP	P1480	–
c.1565G>A	p.Gly522Glu	missense	non trunc	39/282, 790	Perrault et al.[58]	5× P, 1× VUS	LP	M1540	–
c.1648C>T	p.Arg550*	nonsense	truncating	0	–	N	P	PK14085	UK9
c.1653−1G>A	p.Arg551?	splice	truncating	0	–	N	P	M1111	–
c.1655_1656del	p.Glu552fs*6	FS del	truncating	0	Xu et al.[62]	N	P	P1497, 1470059	–
c.1959G>A	p.Trp653*	nonsense	truncating	4/280,738	–	1× P, 1× VUS	LP	–	UK13
c.2278C>T	p.Arg760*	nonsense	truncating	0	Schmidts et al.[59]	1× P	P	F430	UK1
c.2285_2286del	p.Phe762fs*39	FS del	truncating	0	–	N	LP	P1320	–
c.2399+1G>T	p.Ser800?	splice	truncating	14/251, 478	Perrault et al.[58]	5× P	P	M132, M154, M187, M323, M357, P1195, P1504	UK2, UK3, UK6, UK7, UK15, UK18, UK19, UK21, UK22, UK23, UK24, UK27
c.2400−2A>T	p.Ser800?	splice	truncating	0	–	1× P	LP	M1629	–
c.2483delG	p.Gly828fs*18	FS del	truncating	0	–	N	LP	390044	–
c.2500C>T	p.Arg834*	nonsense	truncating	2/256, 536	–	1× P	LP	–	UK8
c.2542_2559del	p.Arg848_Ala853del	IF del	non trunc	0	–	N	LP	PK14084	–
c.2767_2768+2del	p.Tyr923fs*18	splice	truncating	8/148,386	–	2× LP	LP	M199, M1062, M1554	–
c.2909_2920del	p.Glu970_Ala973del	IF del	non trunc	2/281,118	–	N	LP	M120	–

(*Continued on next page*)

Table 2. *Continued*

cDNA variant[a]	Protein variant	Type	Effect	GnomAD v2.1.1	Publication	ClinVar	ACMG designation	Part 1 pedigrees	100,000 Genomes pedigrees
c.2998−1G>A	p.Lys999?	splice	truncating	0	–	N	LP	–	UK20
c.3214C>T	p.Arg1072*	nonsense	truncating	3/249,956	–	N	LP	–	UK5
c.3696del	p.Ile1234Serfs*33	FS del	truncating	0	–	N	LP	PK14083	–

FS del, frameshift deletion; FS dup, frameshift duplication; IF del, inframe deletion; non trunc, nontruncating; P, pathogenic; LP, likely pathogenic, VUS, variant of uncertain significance.
[a]RefSeq transcript GenBank: NM_014714.4.

(Figures 3J–3L). Both had normal kidney function, and the family history was uncertain.

Pedigree 1470059

In this family from the ADPKD Modifier study, the proband (II-1) had large cystic kidneys with a few large cysts and renal insufficiency at 76 years, while his son (III-1) has just a few tiny bilateral cysts (Figures 3M–3O). *IFT140* c.1655_1656del segregated in these individuals.

Pedigree M1169

The proband in this family (II-1) had mild bilateral renal cystic disease and no liver cysts (Figures 3P and 3Q). Her father (I-1) had two left kidney cysts and shared the nonsense variant *IFT140*: c.1377G>A (p.Trp459*) with II-1. The sister II-2 was reported to have bilateral kidney cysts but limited clinical information and no DNA was available (Table S2).

Pedigree M1266

The proband, II-2, had multiple small kidney cysts, some exophytic, and multiple small liver cysts (Figures 3R and 3S), while her sister (II-1) had multiple small kidney cysts, with one larger cyst. Both shared the *IFT140* frameshift variant, c.223delG (p.Val75fs*11).

Singleton individuals with monoallelic *IFT140*-truncating variants

In addition to the multiplex families, 26 families with a single genetically and clinically confirmed case with an *IFT140* pathogenic variant were identified (see Tables 1, 2, and S2 and Figures S1–S3 for details). The majority of these families did not have a known family history, but in seven families, an affected relative was known or suspected, but a sample to test segregation and detailed clinical data was not available (Table S2). In pedigree F392, two relatives had the familial *IFT140* variant but had negative ultrasounds at 53 years and 40 years, and in M241, the son had the family variant, but no clinical information was available. The phenotype in the singleton subjects was consistent with the familial cases; the kidney disease was generally bilateral with variable numbers of large cysts present and few liver cysts (Figures S1–S3). Unlike the multiplex families where all variants were truncating, four singleton cases had non-truncating variants. Two were larger inframe deletions that scored as likely pathogenic by ACMG guidelines (Figures S3G and S3I), and two were missense changes that have previously been scored as likely pathogenic changes associated with SRTD9; including c.634G>A (p.Gly212?), which is a likely splicing variant (Figures S3B, S3C, and S3E; Table 2).

IFT140 pathogenic variants are strongly enriched in cystic kidney families

Our analysis identified 38 families with *IFT140* pathogenic variants, 36 from tNGS, one from WES, and one from WGS (Figure 1). None of these families had an LoF *PKD1* or *PKD2* (or other ADPKD-like gene) variant. Of the previously unscreened families, 16/834 (1.9%) had an *IFT140* pathogenic variant. This compared to 21/381 (5.5%) families for whom no *PKD1* and *PKD2* pathogenic variant had been identified through previous testing (Figure 1).

Genomics England 100K Genomes Project analysis

To determine the burden of likely pathogenic *IFT140* variants more broadly, we analyzed genetic and clinical data from the 100K Genomes Project that includes National Health Service (NHS) subjects affected by a rare disease or cancer and relatives. *IFT140* variants were extracted from WGS of 64,185 subjects and after annotation 26 distinct strongly predicted pathogenic variants (stop gain, start loss, and canonical splice acceptor and donor variants) were identified in a total of 152 individuals (89 probands and 63 relatives) from 111 different families. Among these 152 individuals, kidney cyst(s) were described in 40 individuals (26.3%), including 31/89 probands (34.8%); 27 of these probands were recruited to the 100kG under the "cystic kidney disease" (100kG; PKD) group. Analysis of the 100kG; PKD group showed that 27/1,291 (2.1%) probands had *IFT140* likely pathogenic variants, but these variants were much rarer in probands in other rare disease groups (62/33,127; 0.19%; $p < 0.0001$) or probands with primary neurological diagnoses (18/8,162; 0.22%; $p < 0.0001$). Twenty-five IFT140-positive probands in the 100kG; PKD group were considered unsolved by the Genomics England analysis; two carried monoallelic VUSs in *PKD1* (see Tables 3 and S3). Three families showed segregation of the *IFT140* variant with the cystic phenotype in 3, 2, or 1 family member (Table S3).

UK Biobank analysis

Recently *IFT140*, or the recurrent *IFT140* LoF variant c.2399+1G>T, was suggested to be associated with kidney

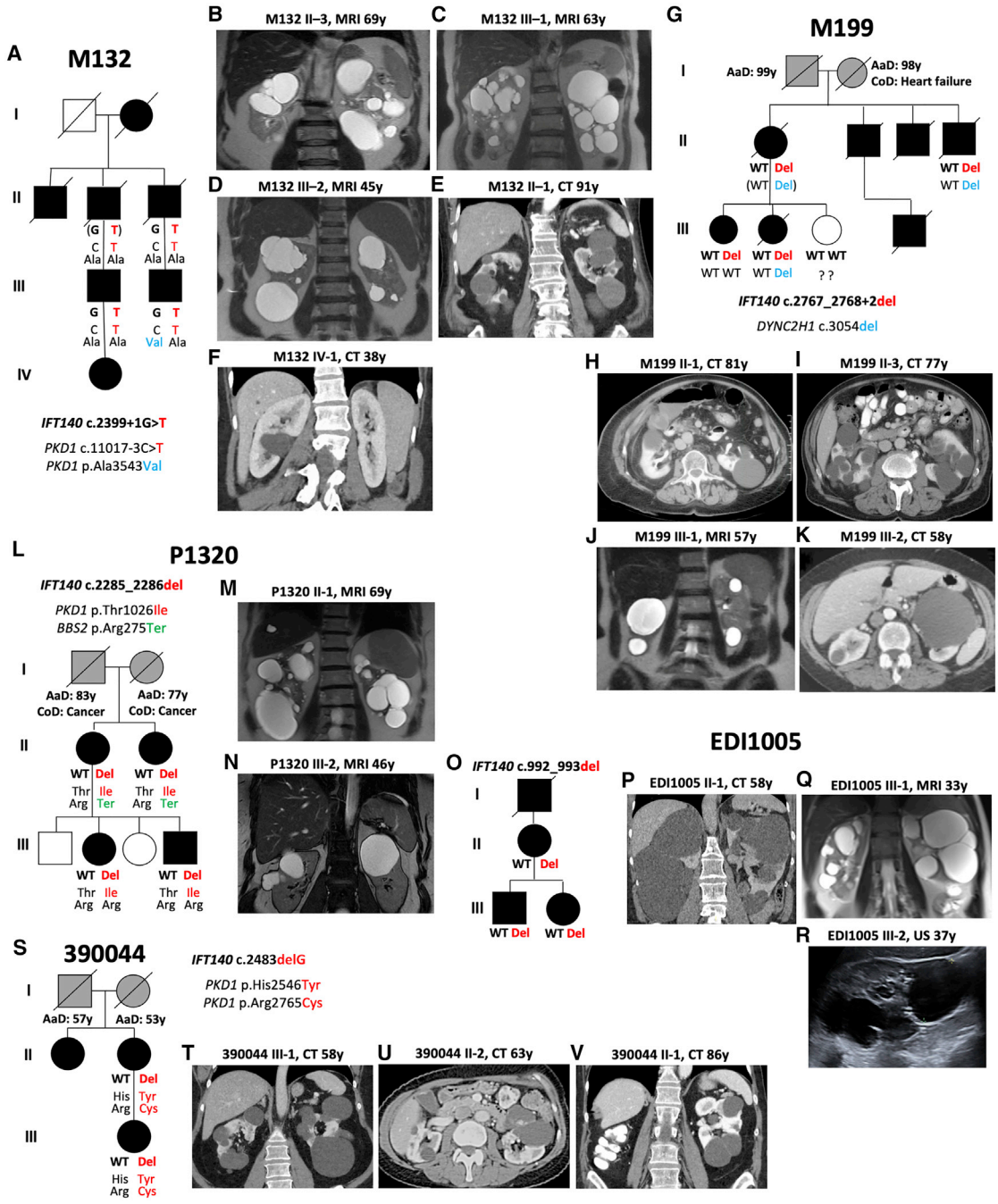

Figure 2. Pedigree and imaging details of five IFT140 pedigrees

(A–V) Pedigrees M132 (A), M199 (G), P1320 (L), EDI1005 (O), and 390044 (S); clinically affected individuals are in black, unaffected are in white, uncertain are in gray, and deceased subjects are lined through. Only affected individuals or others with a sample available are shown. (A) In M132, segregation of the *IFT140* pathogenic variant and *PKD1* VUS are shown; *IFT140*: c.2399+1G>T and *PKD1*: c.11017−3C>T cosegregate. (G) In M199, inheritance of *IFT140*: c.2767_27688+2del and a frameshifting variant in *DYNC2H1* (bi-allelically causing SRTD3), which does not segregate with the disease, are shown. (L) In P1320, the *IFT140* pathogenic variant segregates in four individuals with a *PKD1* VUS, while a *BBS2* nonsense variant does not cosegregate with disease. EDI1005 (O) just had an *IFT140* pathogenic variant. Two *PKD1* VUSs cosegregated with the *IFT140* pathogenic variant in 390044 (S). It is not known whether these additional variants have any influence on the disease phenotype (see Table 3 for details). Abdominal coronal imaging by MRI (B–D, J, M, N, and Q) or CT (E, F, P, T, and V), axial imaging by CT (H, I, K, and U), or abdominal ultrasound (US) (R) with the age at imaging indicated shows the kidney phenotype is typically multiple, larger bilateral cysts, sometimes with marked asymmetry (K). Only M132 IV-1 (F) has liver cysts.

cyst phenotypes in the UK Biobank population and the TOPMed Program.[52,64] UK Biobank subjects were typically between 50 and 75 years old, and the study was not enriched for monogenic disease. A total of 240,037 individuals with WES data were available for study.[52] Genes were screened for enrichment of protein-truncating

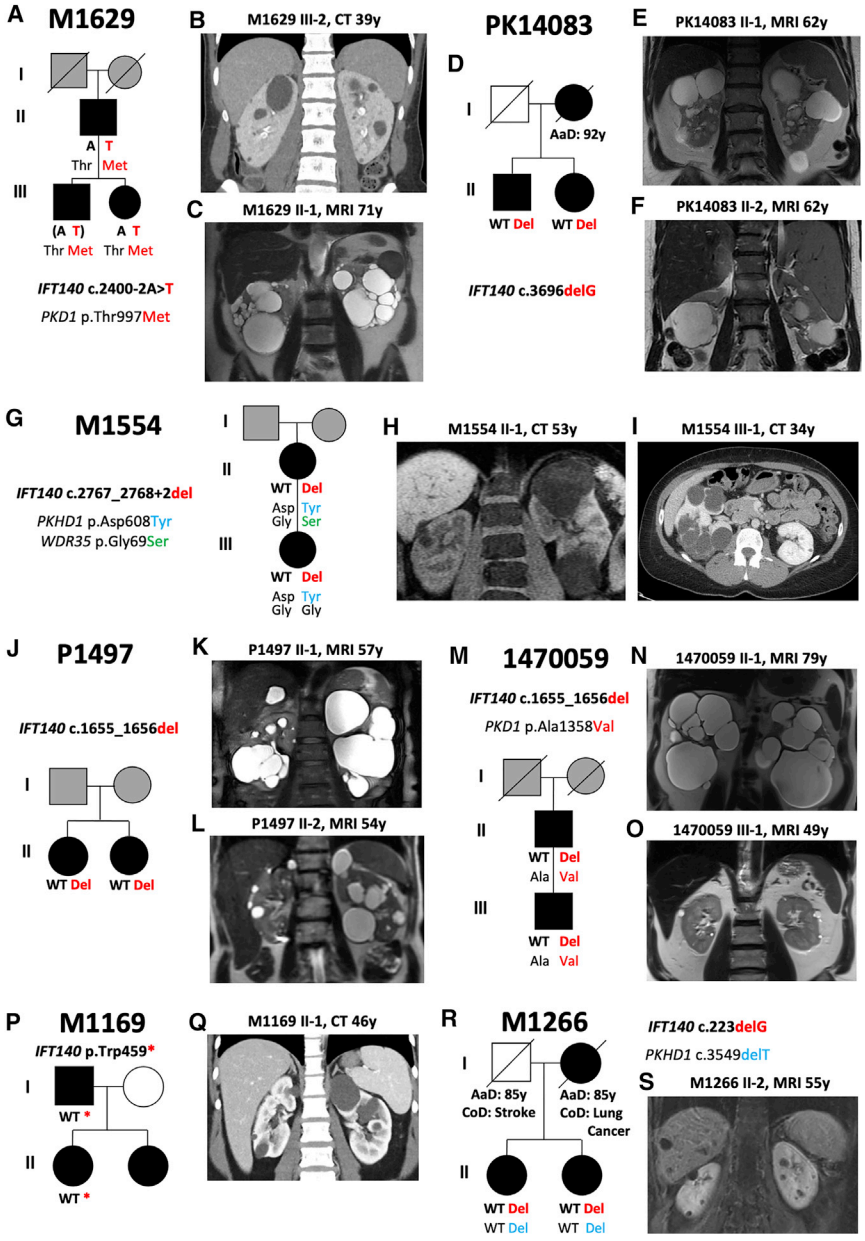

Figure 3. Pedigrees and imaging details of seven IFT140 families

(A–S) Pedigrees of M1629 (A), PK14083 (D), M1554 (G), P1497 (J), 1470059 (M), M1169 (P), and M1266 (R); clinically affected individuals are in black, unaffected are in white, uncertain are in gray, and deceased subjects are lined through. Only affected individuals or others with a sample available are shown. The segregation of the *IFT140* pathogenic variant in each family is shown (inferred in M1629 III-1), plus inheritance of variants in *PKD1*; *in cis* with the *IFT140* pathogenic variant in M1629 and 1470059. A truncating variant or variant of uncertain significance to *PKHD1* (M1554 and M1266), which cosegregate with disease, and *WDR35* (M1554), which does not, are also noted. It is not known if these additional variants have any influence on the disease phenotype (see Table 3 for details). Abdominal coronal MRI (C, E, F, K, L, N, O, and S), coronal (B, H, and Q) or axial CT (I) with the age at imaging indicated shows the kidney and liver phenotypes. The cystic presentation varies from several large cysts bilaterally (N) to much milder cystogenesis (O and S).

variants (including nonsense, canonical splice, or frameshifts) in the ICD-10 code Q61 (cystic kidney disease; n = 521) group compared to controls (without Q61; n = 239,516). Individuals with monoallelic *IFT140*-truncating variants represented 2.69% of Q61 cases compared to 0.21% of controls ($p = 1.62e^{-11}$; Figure 4A). Carriers of truncating variants to *PKD1*, 8.45% cases versus 0.015% controls, and *PKD2*, 5.57% cases versus 0.004% controls, were also, as expected, highly enriched in the PKD group ($p = 3.04e^{-96}$ and $1.63e^{-69}$, respectively). *ALG9*-truncating variant carriers, 0.77% cases and 0.032% controls, were the next highest but not significantly enriched ($p = 0.00003$; significance threshold $p = 1.0e^{-8.7}$).

In a separate analysis of the UK Biobank population, the prevalence of high (likely pathogenic: frameshifting, nonsense, or canonical splicing) versus low impact variants (likely benign: synonymous, non-canonical intronic) with a gnomAD MAF $\leq$ 0.1% were compared for various ICD-10 kidney disease codes (Figure 4B). For this analysis, out of a total population of 200,643 subjects with WES data, 481 individuals were monoallelic for high and 5,888 had low impact *IFT140* variants. ICD-10 codes for cyst of kidney (N28.1), cystic kidney disease (Q61), and CKD stages 4 and 5 (N18.4 and N18.5) were more common in individuals carrying high compared to low impact *IFT140* variants: 2.7% versus 0.5% ($p = 1.3e^{-5}$, OR = 5.3; 95 CI: 2.7–10.1); 1.0% versus 0.07% ($p = 2.4e^{-4}$, OR = 15.4; 95 CI 4.7–50.5); and 1.0% versus 0.3% (p = 0.02, OR = 3.9; 95 CI 1.5–10.3), respectively, whereas other kidney phenotypes were not significant (Figure 4B).

The monoallelic IFT140 phenotype

IFT140 subjects from part 1 of the study typically had conserved renal function, but 32 had an eGFR < 60, and one with a single kidney due to nephrectomy following infantile Wilms tumor had ESKD at 64 years (Tables 1 and S2). A plot of eGFR versus age showed an overall milder disease course than for PKD2 but a lower eGFR than seen in normal individuals (Figure 5A).[65] IFT140 individuals were diagnosed at a mean age of 52.7 years (±13.2 years), compared to 29.9 years (±11.9 years) for

Table 3. Details of other variants of interest

***IFT140* pathogenic variant**	**Gene**	**cDNA variant**[a]	**Protein variant**	**Type**	**Effect**	**CADD score**[b]	**ACMG Des**	**PKD DB**[c]	**GnomAD v2.1.1**	**ClinVar**	**Individuals**	**Pedigree**
c.223delG (p.Val75fs*11)	*PKHD1*	c.3549delT	p.His1184fs*36	FS del	trunc	NA	LP^R	–	0	1× P	II-1, II-2	M1266
c.490G>T (p.Glu164*)	*TMEM231*	c.248C>A	p.Ser83*	nons	trunc	NA	LP^R	–	0	N	10235	F392
c.581delT (p.Leu194fs*2)	*COL4A1*	c.1612C>T	p.Arg538Trp	mis	non trunc	23.9	VUS	–	4/251,364	N	406737	440003
	PKD1	c.2032G>T	p.Ala678Ser	mis	non trunc	4.00	VUS	no	0	N		
	PKD1	c.4055G>A	p.Ser1352Asn	mis	non trunc	14.34	VUS	VUS	186/279,278	1× LB, 2× VUS		
c.594dupG (p.Ser199fs*21)	*PKD1*	c.4055G>A	p.Ser1352Asn	mis	non trunc	14.34	VUS	VUS	186/279,278	1× LB, 2× VUS	R3376	M1374
c.634G>A (p.Gly212?)	*PKD1*	c.8293C>T	p.Arg2765Cys	mis	non trunc	29.20	VUS	M	1299/278,546	1× B, 2× VUS, 2× LP	R3248	M1277
c.1010−1G>A (p.Gly337?)	*PKD1*	c.4963G>A	p.Val1655Met	mis	non trunc	0.05	LB	no	15/279,582	N	10664	F662
	TTC21B	c.2318C>A	p.Ser773*	nons	trunc	NA	LP^R	–	0	N		
c.3214C>T (p.Arg1072*)	*PKD1*	c.3019G>A	p.Val1007Met	mis	non trunc	22.70	VUS	no	5/244,386	1× VUS	*UK5-1*	*UK5*
c.1377G>A (p.Trp459*)	*WDR60*	c.69G>A	p.Trp23*	nons	trunc	N/A	VUS	–	84/248,930	1× P, 2× VUS	R1403	M241
	ALG9	c.551T>G	p.Phe184Cys	mis	non trunc	29.0	VUS	–	18/280,924	N	R1367	M274
	PKD2	c.112G>C	p.Ala38Pro	mis	non trunc	18.48	VUS	no	0	N		
	OFD1	c.936-2A>G	p.Asn313?	splice	trunc	N/A	VUS	–	24/202,878	1× B, 2× VUS	Ox5262	P1505
c.1565G>A (p.Gly522Glu)	*PKHD1*	c.1018G>A	p.Gly340Arg	mis	non trunc	16.58	VUS	–	16/282,680	2× VUS	R2098	M1540
c.1653−1G>A, (p.Arg551?)	*CEP290*	c.1066G>A	p.Gly356Ser	mis	non trunc	31.0	VUS	–	0	N	R2995	M1111
c.1655_1656del (p.Glu552fs*6)	*PKD1*	c.4073C>T	p.Ala1358Val	mis	non trunc	6.77	LB	no	17/279,412	N	II-1, III-1	1470059

(*Continued on next page*)

Table 3. ***Continued***

IFT140 **pathogenic variant**	**Gene**	**cDNA variant**[a]	**Protein variant**	**Type**	**Effect**	**CADD score**[b]	**ACMG Des**	**PKD DB**[c]	**GnomAD v2.1.1**	**ClinVar**	**Individuals**	**Pedigree**
c.2278C>T (p.Arg760*)	*PKD1*	c.113T>A	p.Leu38His	mis	non trunc	22.60	VUS	no	0	N	8143	F430
	TMEM260	c.721dupT	p.Tyr241fs*3	FS dup	trunc	N/A	LP^{R}	–	6/251,474	1× P		
c.2285_2286del (p.Phe762fs*39)	*PKD1*	c.3077C>T	p.Thr1026Ile	mis	non trunc	18.23	LB	LN	12/278,272	N	all	P1320
	BBS2	c.823C>T	p.Arg275*	nons	trunc	N/A	LP^{R}	–	54/282,748	12× P	II-1, II-2	
c.2399+1G>T (p.Ser800?)	*PKD1*	c.11017−3C>T	p.Arg3672?	splice	non trunc	N/A	LB	LN	298/279,962	3× VUS	all R1142 R19	M132 M154 M187
	PKD1	c.10601C>T	p.Ala3534Val	mis	non trunc	18.22	LB	no	43/238,314	N	III-2	M132
	DZIP1L	c.544C>T	p.Arg182Trp	mis	non trunc	31.0	VUS	–	6/278,088	N	R1142	M154
	PKD1	c.8293C>T	p.Arg2765Cys	mis	non trunc	29.20	VUS	M	1299/278,546	1× B, 2× VUS, 2× LP	R1606	M323
	IFT43	c.343C>T	p.Gln115*	nons	trunc	N/A	LP^{R}	–	12/282,886	N	Ox5058	P1504
	PKD1	c.360−5T>G	p.Ile120?	splice	non trunc	N/A	VUS	no	0	N	*UK27-1*	*UK27*
c.2400−2A>T (p.Ser800?)	*PKD1*	c.2990C>T	p.Thr997Met	mis	non trunc	23.60	VUS	no	2/240,882	N	II-1, III-1, III-2	M1629
c.2483delG (p.Gly828fs*18)	*PKD1*	c.8293C>T	p.Arg2765Cys	mis	non trunc	29.20	VUS	M	1299/278,546	1× B, 2× VUS, 2× LP	II-1, III-1	390044
	PKD1	c.7636C>T	p.His2546Tyr	mis	non trunc	17.69	VUS	LN	411/251,160	2× B, 1× LB, 1× VUS		
c.2767_2768+2del (p.Tyr923fs*18)	*DYNC2H1*	c.3054delT	p.Phe1018fs*3	FS del	trunc	N/A	LP^{R}	–	0	N	II-1, II-4, III-2	M199
	PKD1	c.2098−3C>T	p.Val700?	splice	non trunc	N/A	LB	no	7/133,582	LB	R2939	M1062
	PKHD1	c.1822G>T	p.Asp608Tyr	mis	non trunc	21.8	VUS	–	1/246,468	N	II-1, III-1	M1554
	WDR35	c.205G>A	p.Gly69Ser	mis	non trunc	28.0	VUS	–	0	N	II-1	

FS del, frameshift deletion; Nons, nonsense; Mis, missense; FS dup, frameshift duplication; non trunc, nontruncating; NA, not applicable; ACMG Des, designation; P, pathogenic; LP, likely pathogenic; VUS, variant of uncertain significance; LB, likely benign; B, benign; ^{R}, designation associated with bi-allelic status; M, possible modifying allele; LN, likely neutral.

[a]RefSeq transcripts *ALG9*, GenBank: NM_024740; *BBS2*, GenBank: NM_031885; *CEP290*, GenBank: NM_025114; *COL4A1*, GenBank: NM_001845; *DYNC2H1*, GenBank: NM_001080463; *DZIP1L*, GenBank: NM_173543; *IFT43*, GenBank: NM_052873; *OFD1*, GenBank: NM_003611; *PKD1*, GenBank: NM_001009944; *PKD2*, GenBank: NM_000297; *PKHD1*, GenBank: NM_138694; *TMEM231*, GenBank: NM_001077416; *TMEM260*, GenBank: NM_017799; *TTC21B*, GenBank: NM_024753; *WDR35*, GenBank: NM_001006657; *WDR60*, GenBank: NM_018051.

[b]Higher scores indicate a higher probability of pathogenicity.

[c]The ADPKD Mutation Database.

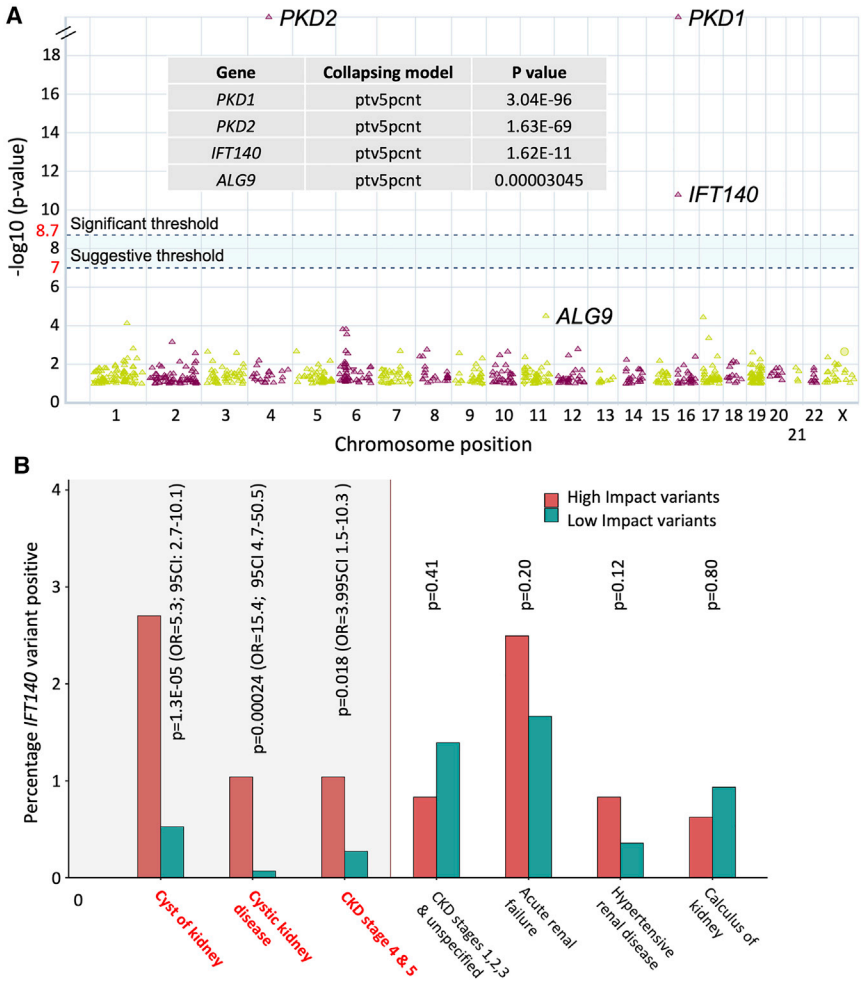

Figure 4. UK Biobank data demonstrate *IFT140* LoF alleles are associated with cystic kidney disease

(A) Gene-level Manhattan association plot with binary trait Q61 (cystic kidney disease) and Fisher's exact two-sided test statistics. A significance threshold of $P \leq 2 \times 10^{-9}$ has been selected (see subjects and methods). Here, gene-level results are shown with a collapsing model based on protein-truncating variants with a gnomAD MAF of ≤5% (ptv5pcnt). The proportion of cases with a qualifying protein-truncating variants in the Q61 group (n = 521) was compared with the proportion in controls (n = 239,516) for each gene. Among the 521 cases, 14 (2.69%) had a monoallelic *IFT140*-truncating variant, compared to 506 (0.21%) among the controls. For *PKD1*, *PKD2*, and *ALG9*, 44 (8.45%) cases and 35 (0.015%) controls, 29 (5.57%) cases and ten (0.004%) controls, and four (0.77%) cases and 76 (0.032%) controls had a monoallelic truncating variant, respectively. The −log10 p values for enrichment in the cystic kidney disease group are shown; *ALG9* did not reach the significance threshold. Graph generated from the Astra Zeneca PheWAS Portal.[52]

(B) Prevalence of kidney-related diagnoses in *IFT140* high (likely pathogenic) versus low impact (likely benign) variant carriers. Of the 200,643 individuals from the UK Biobank with exome data, 481 had monoallelic high and 5,888 low impact variants to *IFT140*. Comparison of individuals with kidney-related diagnoses (grouped by ICD-10 terms) showed that cyst of kidney (N28.1), cystic kidney disease (Q61), and CKD stages 4 and 5 (N18.4 & N18.5) were significantly more common in individuals with high impact *IFT140* variants compared to low impact (shaded; see figure for p values and odds ratios with 95% confidence intervals [CIs]). One high impact carrier was in both the N28.1 and Q61 groups. Other kidney phenotypes were not enriched for high impact *IFT140* variants.

the ADPKD individuals in the TAME study,[66] and the diagnosis was often made incidentally. Hypertension was diagnosed in 66.1% of individuals (where the information was available), with an average age at onset of 56.9 years (the precise age at onset was not present in 14 individuals, and the mean eliminating those was 53.6 years); only one affected individual was hypertensive before 40 years. Therefore, hypertension was less frequent and diagnosed approximately 20 years later than in ADPKD overall.[67] Six IFT140-affected individuals had a vascular phenotype, including intracranial or aortic aneurysm, and some of these individuals had additional PKD gene variants (Table 3), but further study will be required to see whether there is an association as found in ADPKD overall.[4,5] The htTKV was often enlarged in the monoallelic *IFTI40* subjects but asymmetry was common with a small number of cysts accounting for most of the cystic disease (and increased TKV), hence, 27 individuals were classified as having an atypical (2A) MIC.[8] Plotting the htTKV data shows a wide spread of values both for those with a typical and atypical MIC (Figure 5B). Liver cysts were rare, found in only nine subjects and, when present, were usually small (Table 1).

Retinal degeneration is a phenotype associated with biallelic *IFT140* pathogenic variants and there was some anecdotal analysis of eye disease in monoallelic individuals. In M199, III-1 had age-related macular degeneration (AMD) and early-stage retinal pigment epithelium (RPE) detachment, while in M1374, R3376 had AMD and atrophy of the RPE (Table S2; Figure S4). In addition, in P1505, Ox5262 had congenital aniridia and blindness (see also below). However, only a limited number of eye exams were available and analyses in these individuals by an optometrist revealed no systematic eye phenotype. In addition, several individuals had a diagnosis of cancer, including five with colorectal cancer but further analysis will be required to determine whether there is any association. Of note in the 100kG data, nine high impact *IFT140* variant carriers had diaphragmatic (or umbilical) hernias, seven of whom also had kidney cysts, while in the UK Biobank data, ICD-10 K40.9 (unilateral or unspecified inguinal hernia, without obstruction or

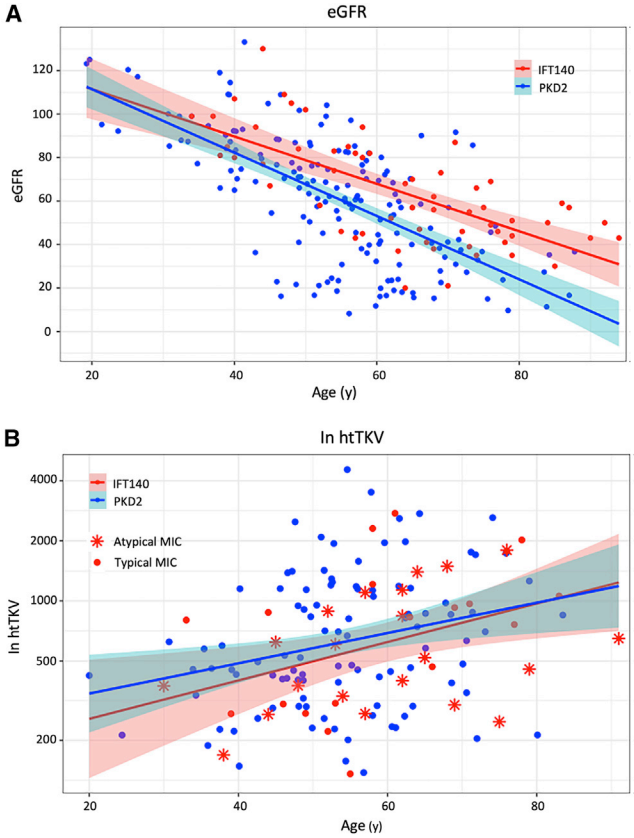

Figure 5. Comparison of eGFR and htTKV between IFT140 and PKD2 individuals

(A) Plotting of eGFR values versus age demonstrates that IFT140 individuals have a slower decline in renal function compared to PKD2[8,9] but quicker than would be expected with normal aging. Only one IFT140 subject reached ESKD and one had CKD stage 4. (B) Plot of height-adjusted TKV on the natural log scale (ln htTKV) versus age for individuals with a typical and atypical MIC differentiated compared to PKD2.[8,9] A wide range of htTKV are seen associated with ADPKD-*IFT140*. Shading shows the 95% confidence intervals.

gangrene) was enriched in high impact carriers ($p = 0.016$).

Genetic variants in other genes

IFT140 lies in chromosome region 16p13.3 (Chr16: 1,560,428–1,662,111; hg19) less than 0.5 Mb distal to *PKD1* (Chr16: 2,138,711–2,185,899; hg19). Consequently by linkage analysis, *IFT140* pathogenic variants can be linked to *PKD1* variants in family and sometimes population analyses. For instance, three families with *IFT140*: c.2399+1G>T also had the *PKD1* variant c.11017−3C>T; these variants co-segregated with the disease in M132 (Figure 2A, Table 3). This *PKD1* noncanonical splicing change has been described as pathogenic but is not predicted to significantly alter splicing and is found 298 times in gnomAD.[68] As another example, *PKD1*: c.2990C>T (p.Thr997Met), a somewhat conservative substitution at a residue well conserved in *PKD1* orthologs, but not in the PKD repeat domain, and found twice in gnomAD, was considered pathogenic from clinical testing because it segregated in three affected individuals in M1629, but *IFT140*: c.2400−2A>T also segregates in this family (Figure 3A). Variants of possible significance in other PKD genes were also found in IFT140 families. For instance, M1266 has the *PKHD1* frameshifting variant c.3549delT (p.His1184fs*36), as well as *IFT140*: c.223delG, both segregating in the two affected sisters and perhaps associated with the liver cysts. Families P1504 and F662 had an LoF variant in another IFT-A encoding gene, *IFT43* (MIM: 614068) or *TTC21B* (MIM: 612014), respectively, and R1403 (M241) had a single LoF to the SRTD gene, *WDR60* (MIM: 615462). LoF variants in three other ciliopathy genes were found in three other families (Table 3), but some variants, *BBS2* (MIM: 606151): c. 823C>T (p.Arg275*) (M1320; Figure 2L) and *DYNC2H1* (MIM: 603297): c.3054delC (p.Phe1018fs*3) (M199; Figure 2G), did not fully segregate with the disease. P1505 had the *OFD1* (MIM: 300171) canonical splicing variant c.936−2A>G, but which is present 24 times in gnomAD and the significance is uncertain. The eye phenotype in this family could be associated with the *IFT140* and/or *OFD1* variants.

Discussion

We provide overwhelming evidence that monoallelic *IFT140* LoF variants cause an ADPKD-like phenotype. Given the phenotypic and genotypic variability associated with monoallelic causes of cystic kidney disease (*PKD1*, *PKD2*, *GANAB*, *DNAJB11*, *ALG9*, etc.), and the familiarity with the ADPKD term by nephrologists and affected individuals, we suggest calling this group of disorders the ADPKD-spectrum and adding the affected gene as a suffix to better describe the disease (i.e., ADPKD-*PKD1* or ADPKD-*IFT140*).[7] Our data comes from family-based and population studies. The families include 12 multiplex pedigrees where segregation was demonstrated or inferred in 33 family members with seven other likely affected family members and in 26 singletons, seven of whom had relatives with kidney cysts. In total, ADPKD-*IFT140* represented 1.9% of naive screened families and 5.5% of those for whom previous testing did not identify *PKD1* or *PKD2* pathogenic variants, with c.2399+1G>T a relatively common pathogenic variant. WES as well as tNGS was employed for screening, and no ADPKD-*IFT140* families had LoF variants to *PKD1*, *PKD2*, or other ADPKD-spectrum genes. Of note, families were identified in clinical trials (HALT PKD, DIPAK RCT, and TAME) and observational studies (CRISP, ADPKD Modifier, Genkyst, DIPAK Observational), where a clinical diagnosis of ADPKD was required for recruitment. In one family, two individuals had the familial *IFT140* pathogenic variant, but kidney cysts were not detected. However, only abdominal ultrasound imaging was available that has lower resolution than MRI or CT. The negative imaging most likely reflects the reduced

penetrance of ADPKD-*IFT140* compared to ADPKD-*PKD1* or ADPKD-*PKD2*, similar to the ADPLD genes where affected individuals may live to old age without a diagnosis unless appropriate imaging is performed.[69]

The population data, both from the 100kG; PKD cohort and UK Biobank, support I*FT140* as a significant ADPKD-spectrum gene. *IFT140* accounted for 2.1% of the 100kG; PKD cohort, none of which had LoF *PKD1* or *PKD2* variants. In the UK Biobank ICD-10 code Q61 cystic kidney disease cohort *IFT140* was identified as the 3rd most enriched ADPKD-spectrum gene. Due to the recruitment criteria, this cohort is likely enriched for milder PKD subjects, but nevertheless, no other gene apart from *PKD1* and *PKD2* was significantly associated with this group. This is consistent with the larger number of identified IFT140 pedigrees described here than for any other ADPKD-spectrum gene, apart from *PKD1* and *PKD2*.[11–14,17,22,70–73] The phenotype is also very consistent, reflective of a monogenic disease; a few large kidney cysts resulting in increased htTKV, renal insufficiency just in older individuals but rarely ESKD, and liver cysts rare or not present. Nevertheless, UK Biobank participants with *IFT140* LoF variants were enriched for CKD 4 and 5, indicating that it is not an entirely benign phenotype.

Although monoallelic *IFT140* pathogenic variants rarely cause ESKD, defining this ADPKD-spectrum gene is important for diagnostics and prognostics. This diagnosis can differentiate a family from ones with *PKD1*, *PKD2*, or *DNAJB11* variants, where the chance of ESKD is much greater. Therefore, an IFT140 diagnosis may be reassuring, although if extrarenal phenotypes are associated with *IFT140*, haploinsufficiency needs further study in larger populations and 100kG and UK Biobank data. The significant number of IFT140 individuals with additional variants to *PKD1*, *PKHD1*, or other ciliopathy genes emphasizes that the IFT140 phenotype may be modified by coinheritance of variants in these other cystogenes. Along with reduced penetrance, genetic modification may explain some of the intrafamilial phenotypic variability. Animal studies and human observations indicate that variants in more than one PKD/PLD gene can combine to accentuate the phenotype.[74–78] Given the close localization of *IFT140* and *PKD1* in 16p13.3, a *PKD1* modifying variant may co-segregate in multiple affected individuals, and *PKD1* analysis alone may misdiagnose the modifying variant as disease causing. Therefore, screening *IFT140* along with *PKD1* and other ADPKD-spectrum genes is important to achieve an accurate molecular diagnosis. The mild phenotype and likely effect of disease modifiers may explain why ADPKD-*IFT140* has hitherto remained unrecognized. Population studies by imaging have identified quite large populations with probable and possible ADPKD, which may partly be accounted for by *IFT140* variants.[3] Interestingly in the UK Biobank, *IFT140* LoF variants were associated with ICD-10 code N-28.1, cyst of kidney. This code includes a small number of "simple" cysts or supposed acquired cystic disease, but our work indicates that some of this group have a monogenic cause.

Kidney size, categorized by htTKV/age into five typical MIC (A–E), is a strong predictor of future decline in renal function in ADPKD.[8,9] For some ADPKD-spectrum genes, such as *DNAJB11*, ESKD can occur without kidney enlargement due to fibrosis; many affected individuals have the atypical, atrophic MIC, 2B, and htTKV/age is not a good predictor of future kidney function.[17] ADPKD-*IFT140* individuals often have enlarged kidneys due to a few large cysts, sometimes resulting in asymmetry and often being categorized as an atypical presentation due to just a few cysts accounting for a large proportion of the TKV (MIC, 2A). However, even if the individual is assigned to a typical MIC, because of the enlargement due to a few large cysts and likely preserved parenchyma, the MIC is not predictive of future renal insufficiency. For ADPKD-spectrum genes, especially beyond *PKD1* and *PKD2*, the addition of genetic data better allows the interpretation of imaging results.[9]

As seen for *IFT140*, there are precedents for bi-allelic disruption of ADPKD-spectrum genes being associated with viable but more severe phenotypes, including kidney cysts. Bi-allelic pathogenic variants to *PKD1* and probably *PKD2*, where at least one variant is hypomorphic, can be associated with very early onset PKD, similar to ARPKD.[79–81] Monoallelic *PKHD1* pathogenic variants can be associated with mild PKD/PLD, and recently bi-allelic *DNAJB11* variants have been associated with an ARPKD-like disease with pancreatic cysts.[14,25,82,83] Bi-allelic variants to *ALG9*, or the ADPLD-associated *ALG8* (MIM: 608103), cause congenital defects of glycosylation (CDG1L and CDG1H, respectively), that involve cystic kidneys as part of severe, developmental disorders.[84,85] In many of these disorders, including the association of bi-allelic *IFT140* variants with SRTD, two LoF variants are probably not compatible with life (viable individuals have at least one nontruncating variant).[58,59,86–88] It therefore follows that these ADPKD-spectrum subjects are unusually vulnerable to cyst development from ADPKD gene dosage reduction.

There has long been rigorous debate about the mechanism of disease in ADPKD, with just a single germline mutation required for cysts development. The detection of somatic mutations to the germline gene in cyst linings, and that induced loss of *Pkd1* or *Pkd2* in the kidney results in cyst development, support a two-hit model of cyst initiation.[89–91] However, bi-allelic disease, that cysts can develop when PC1 is present, and the link between severity of kidney disease and the level of functional PC1 suggest a dosage/threshold model of cystogenesis.[88,92–94] The mechanism of cyst development associated with monoallelic *IFT140* pathogenic variants is not known, but the small number of cysts present could be compatible with a two-hit model. Interestingly, larger deletion somatic events (loss of heterozygosity [LOH]) may also delete *PKD1*, resulting in a dosage loss that may further promote

cyst development/expansion. Likewise, *PKD1* somatic LOH may include deletion of an *IFT140* allele.[95] However, since the tuberous sclerosis gene, *TSC2* (MIM: 191092), lies between *PKD1* and *IFT140*, germline deletions including both genes would result in the more rapidly progressive cystic disease plus TSC phenotypes of the *PKD1-TSC2* contiguous gene syndrome.[96,97]

The previously described minor ADPKD-spectrum and most ADPLD proteins are involved in protein folding and trafficking in the ER, with PC1 an identified protein particularly sensitive to dosage reduction of these proteins resulting in reduced surface and ciliary localization of the PC-complex.[11–14,76] However, here we implicate a protein involved in ciliary structure and function as an ADPKD-spectrum gene. This is important because although loss or disruption of ciliary function has been associated with a cystic phenotype, as part of a syndromic ciliopathy phenotype or in experimental models, in monoallelic human disease it has not been directly shown to cause cyst formation. Indeed, there has been debate whether additional cystogenic factors other than the PC complex and FPC promote cyst formation and/or the NPHP phenotype.[10] The cystogenic effect of *IFT140* haploinsufficiency also seems unusual, since although other IFT-A or SRTD genes were found as modifiers (Table 3), our screening did not indicate any as common monoallelic causes of the ADPKD spectrum.

It is not known whether a 50% dosage reduction of IFT140 results in changes in ciliary structure/function, but the documented null phenotype is greatly shortened cilia with a bulbous tip, illustrating its role in retrograde IFT.[63] However, the IFT-A complex has also been implicated in the regulation of protein localization and gating of the ciliary transition zone during ciliary assembly.[33,56,57] In human cells, loss of the core IFT-A complex protein WDR19 (IFT144) results in failed ciliary entry of the IFT-A complex and membrane proteins and accumulation of IFT-B complex proteins at the bulbous tip.[55] In Chlamydomonas, analysis of truncated IFT140, missing the critical WD repeats, demonstrated improper localization of multiple membrane-bound ciliary proteins.[57] While in *C. elegans*, IFT140 has a role in restricting entry of ciliary membrane proteins, whereas the peripheral IFT-A proteins have been implicated in protein removal from cilia.[56] Since PC1, PC2, and FPC are ciliary localized membrane cystoproteins, and the trafficked level of PC1, at least, seems critical for preventing cystogenesis, subtle reductions of ciliary entry of PC1 (and PC2 and FPC) may underlie cyst development in monoallelic IFT140 subjects. However, further structural and functional analysis of IFT140$^{+/-}$ cilia is required to better understand cystogenesis in this setting.

In conclusion, monoallelic LoF *IFT140* variants result in an atypical, mild form of ADPKD, consisting of large bilateral cysts and renal functional decline in older ages. *IFT140* likely represents >1% of ADPKD-spectrum-affected individuals and is found in many studied ADPKD cohorts. Association of an IFT-complex protein with the ADPKD spectrum strengthens the link between ciliary defects and ADPKD and may help understand pathogenesis in the wider group of ADPKD-spectrum disorders.

Data and code availability

Primary data from the 100,000 Genomes Project, which are held in a secure research environment, are available to registered users. UK Biobank association statistics are publicly available through the AstraZeneca Centre for Genomics Research (CGR) PheWAS Portal. UK Biobank whole-exome sequencing data described in this paper are publicly available to registered researchers through the UKB data access protocol.

Supplemental information

Supplemental information can be found online at https://doi.org/10.1016/j.ajhg.2021.11.016.

Acknowledgments

We thank the families and coordinators for involvement in the study and Saurabh Baheti (Mayo Clinic), Dana Miskulin (Tufts University), Susan L. Murray (Beaumont Hospital, Dublin), Aurore Despres and Christelle Guillerm (CHU Brest), Aude Promerat and Cécile Lemoine (Roubaix), Anne-Laure Faucon (Corbeil-Essone), Emad Khazned (Bourges), Alain Michel (Saint Malo), Charles J. Blijdorp (Erasmus Medical Center, Rotterdam), Rene M.M. van Aerts (University Medical Center Radboud, Nijmegen), and Shosha E.I. Dekker (Leiden University Medical Center) for technical assistance or referring individuals. This research was conducted with data from UK Biobank (project ID 43879) and data and findings from the 100,000 Genomes Project. The study was supported by NIDDK grants DK058816 and DK059597 (P.C.H.); the Mayo Translational PKD Center (DK090728; V.E.T.); the Zell Family Foundation, Robert and Billie Kelley Pirnie, an Early Postdoc Mobility Stipendium, Swiss National Science Foundation (P2ZHP3_195181), and Kidney Research UK (Paed_RP_001_20180925) (E.O.); Kidney Research UK and the Northern Counties Kidney Research Fund (J.A.S.); a Barbour Foundation Postgraduate Research Studentship (R.P.); and Kuwait Foundation for the Advancement of Sciences (KFAS) grant PR17-13MM-07 (H.O.). The Irish Kidney Gene Project was funded by THE HEALTH RESEARCH BOARD, Irish Nephrology Society, Irish Kidney Association under the HRCI-HRB Joint Funding Scheme HRCI-HRB-2020-032; the Baltimore PKD Research and Clinical Core Center were supported by P30DK090868 and U54 DK126114. Support for HALT PKD, CRISP, the ADPKD Modifier Study, Genkyst, DIPAK, the UK Biobank, and the 100,000 Genomes Project are shown in the supplemental materials, along with additional investigators from these studies.

Declaration of interests

M.M. reports grants and consulting fees outside the submitted work from Otsuka Pharmaceuticals, Sanofi, Chinook, Goldilocks, Natera, and Palladio. R.D.P. reports clinical trial support from Reata, Kadmon, Sanofi-Genzyme, US Department of Defense; consultant/advisory fees from Otsuka and Sanofi-Genzyme; and is section editor Renal Cystic Disease: UpToDate. J.A.S. has

received honorarium from consulting positions from Otsuka Pharmaceuticals, Sanofi, and Takeda. V.E.T. reports grants and/or other fees from Mironid, Blueprint Medicines, Otsuka Pharmaceuticals, Palladio Biosciences, Sanofi Genzyme, Reata, and Regulus Therapeutics, all outside the submitted work.

Received: October 1, 2021
Accepted: November 15, 2021
Published: December 9, 2021

Web resources

ACMG Calculator, https://www.medschool.umaryland.edu/genetic_variant_interpretation_tool1.html/
ADPKD Mutation Database (PKD DB), https://pkdb.mayo.edu/
AstraZeneca PheWAS Portal, https://azphewas.com/
ClinVar, https://www.ncbi.nlm.nih.gov/clinvar/
Ensembl Genome Browser, https://useast.ensembl.org/index.html
Genomics England 100K Project, https://www.genomicsengland.co.uk/
GnomAD Browser, https://gnomad.broadinstitute.org/
IMPACT predictions, Ensembl Variation - Calculated variant consequences, https://www.ensembl.org/info/genome/variation/prediction/predicted_data.html
Mayo Imaging Class, https://www.mayo.edu/research/documents/pkd-center-adpkd-classification/doc-20094754
NCBI Nucleotide, https://www.ncbi.nlm.nih.gov/nuccore
OMIM, http://www.omim.org
RefSeq, https://www.ncbi.nlm.nih.gov/refseq/
SnpEff variant annotations, http://pcingola.github.io/SnpEff/
UCSC Genome Browser, https://genome.ucsc.edu
UK Biobank, https://www.ukbiobank.ac.uk/
UK Biobank showcase portal, https://biobank.ndph.ox.ac.uk/showcase/label.cgi?id=170

References

1. Cornec-Le Gall, E., Alam, A., and Perrone, R.D. (2019). Autosomal dominant polycystic kidney disease. Lancet *393*, 919–935.
2. Bergmann, C., Guay-Woodford, L.M., Harris, P.C., Horie, S., Peters, D.J.M., and Torres, V.E. (2018). Polycystic kidney disease. Nat. Rev. Dis. Primers *4*, 50.
3. Suwabe, T., Shukoor, S., Chamberlain, A.M., Killian, J.M., King, B.F., Edwards, M., Senum, S.R., Madsen, C.D., Chebib, F.T., Hogan, M.C., et al. (2020). Epidemiology of Autosomal Dominant Polycystic Kidney Disease in Olmsted County. Clin. J. Am. Soc. Nephrol. *15*, 69–79.
4. Hogan, M.C., Abebe, K., Torres, V.E., Chapman, A.B., Bae, K.T., Tao, C., Sun, H., Perrone, R.D., Steinman, T.I., Braun, W., et al. (2015). Liver involvement in early autosomal-dominant polycystic kidney disease. Clin. Gastroenterol. Hepatol. *13*, 155–64.e6.
5. Sanchis, I.M., Shukoor, S., Irazabal, M.V., Madsen, C.D., Chebib, F.T., Hogan, M.C., El-Zoghby, Z., Harris, P.C., Huston, J., Brown, R.D., and Torres, V.E. (2019). Presymptomatic Screening for Intracranial Aneurysms in Patients with Autosomal Dominant Polycystic Kidney Disease. Clin. J. Am. Soc. Nephrol. *14*, 1151–1160.
6. Heyer, C.M., Sundsbak, J.L., Abebe, K.Z., Chapman, A.B., Torres, V.E., Grantham, J.J., Bae, K.T., Schrier, R.W., Perrone, R.D., Braun, W.E., et al. (2016). Predicted Mutation Strength of Nontruncating PKD1 Mutations Aids Genotype-Phenotype Correlations in Autosomal Dominant Polycystic Kidney Disease. J. Am. Soc. Nephrol. *27*, 2872–2884.
7. Cornec-Le Gall, E., Torres, V.E., and Harris, P.C. (2018). Genetic Complexity of Autosomal Dominant Polycystic Kidney and Liver Diseases. J. Am. Soc. Nephrol. *29*, 13–23.
8. Irazabal, M.V., Rangel, L.J., Bergstralh, E.J., Osborn, S.L., Harmon, A.J., Sundsbak, J.L., Bae, K.T., Chapman, A.B., Grantham, J.J., Mrug, M., et al. (2015). Imaging classification of autosomal dominant polycystic kidney disease: a simple model for selecting patients for clinical trials. J. Am. Soc. Nephrol. *26*, 160–172.
9. Lavu, S., Vaughan, L.E., Senum, S.R., Kline, T.L., Chapman, A.B., Perrone, R.D., Mrug, M., Braun, W.E., Steinman, T.I., Rahbari-Oskoui, F.F., et al. (2020). The value of genotypic and imaging information to predict functional and structural outcomes in ADPKD. JCI Insight *5*, e138724.
10. Ma, M., Gallagher, A.R., and Somlo, S. (2017). Ciliary Mechanisms of Cyst Formation in Polycystic Kidney Disease. Cold Spring Harb. Perspect. Biol. *9*, a028209.
11. Porath, B., Gainullin, V.G., Cornec-Le Gall, E., Dillinger, E.K., Heyer, C.M., Hopp, K., Edwards, M.E., Madsen, C.D., Mauritz, S.R., Banks, C.J., et al. (2016). Mutations in GANAB, Encoding the Glucosidase IIα Subunit, Cause Autosomal-Dominant Polycystic Kidney and Liver Disease. Am. J. Hum. Genet. *98*, 1193–1207.
12. Cornec-Le Gall, E., Olson, R.J., Besse, W., Heyer, C.M., Gainullin, V.G., Smith, J.M., Audrézet, M.P., Hopp, K., Porath, B., Shi, B., et al. (2018). Monoallelic Mutations to DNAJB11 Cause Atypical Autosomal-Dominant Polycystic Kidney Disease. Am. J. Hum. Genet. *102*, 832–844.
13. Besse, W., Chang, A.R., Luo, J.Z., Triffo, W.J., Moore, B.S., Gulati, A., Hartzel, D.N., Mane, S., Torres, V.E., Somlo, S., Mirshahi, T.; and Regeneron Genetics Center (2019). *ALG9* Mutation Carriers Develop Kidney and Liver Cysts. J. Am. Soc. Nephrol. *30*, 2091–2102.
14. Besse, W., Dong, K., Choi, J., Punia, S., Fedeles, S.V., Choi, M., Gallagher, A.R., Huang, E.B., Gulati, A., Knight, J., et al. (2017). Isolated polycystic liver disease genes define effectors of polycystin-1 function. J. Clin. Invest. *127*, 1772–1785.
15. Drenth, J.P., te Morsche, R.H., Smink, R., Bonifacino, J.S., and Jansen, J.B. (2003). Germline mutations in *PRKCSH* are associated with autosomal dominant polycystic liver disease. Nat. Genet. *33*, 345–347.
16. Li, A., Davila, S., Furu, L., Qian, Q., Tian, X., Kamath, P.S., King, B.F., Torres, V.E., and Somlo, S. (2003). Mutations in PRKCSH cause isolated autosomal dominant polycystic liver disease. Am. J. Hum. Genet. *72*, 691–703.
17. Huynh, V.T., Audrézet, M.P., Sayer, J.A., Ong, A.C., Lefevre, S., Le Brun, V., Després, A., Senum, S.R., Chebib, F.T., Barroso-Gil, M., et al. (2020). Clinical spectrum, prognosis and estimated prevalence of DNAJB11-kidney disease. Kidney Int. *98*, 476–487.
18. Devuyst, O., Olinger, E., Weber, S., Eckardt, K.U., Kmoch, S., Rampoldi, L., and Bleyer, A.J. (2019). Autosomal dominant tubulointerstitial kidney disease. Nat. Rev. Dis. Primers *5*, 60.
19. Hu, J., and Harris, P.C. (2020). Regulation of polycystin expression, maturation and trafficking. Cell. Signal. *72*, 109630.
20. Izzi, C., Dordoni, C., Econimo, L., Delbarba, E., Grati, F.R., Martin, E., Mazza, C., Savoldi, G., Rampoldi, L., Alberici, F., and Scolari, F. (2020). Variable Expressivity of HNF1B Nephropathy, From Renal Cysts and Diabetes to Medullary

Sponge Kidney Through Tubulo-interstitial Kidney Disease. Kidney Int. Rep. *5*, 2341–2350.
21. Gulati, A., Bae, K.T., Somlo, S., and Watnick, T. (2018). Genomic Analysis to Avoid Misdiagnosis of Adults With Bilateral Renal Cysts. Ann. Intern. Med. *169*, 130–131.
22. Schönauer, R., Baatz, S., Nemitz-Kliemchen, M., Frank, V., Petzold, F., Sewerin, S., Popp, B., Münch, J., Neuber, S., Bergmann, C., and Halbritter, J. (2020). Matching clinical and genetic diagnoses in autosomal dominant polycystic kidney disease reveals novel phenocopies and potential candidate genes. Genet. Med. *22*, 1374–1383.
23. Gulati, A., Sevillano, A.M., Praga, M., Gutierrez, E., Alba, I., Dahl, N.K., Besse, W., Choi, J., and Somlo, S. (2019). Collagen IV Gene Mutations in Adults With Bilateral Renal Cysts and CKD. Kidney Int. Rep. *5*, 103–108.
24. Cornec-Le Gall, E., Chebib, F.T., Madsen, C.D., Senum, S.R., Heyer, C.M., Lanpher, B.C., Patterson, M.C., Albright, R.C., Yu, A.S., Torres, V.E., Harris, P.C.; and HALT Progression of Polycystic Kidney Disease Group Investigators (2018). The Value of Genetic Testing in Polycystic Kidney Diseases Illustrated by a Family With PKD2 and COL4A1 Mutations. Am. J. Kidney Dis. *72*, 302–308.
25. Gunay-Aygun, M., Turkbey, B.I., Bryant, J., Daryanani, K.T., Gerstein, M.T., Piwnica-Worms, K., Choyke, P., Heller, T., and Gahl, W.A. (2011). Hepatorenal findings in obligate heterozygotes for autosomal recessive polycystic kidney disease. Mol. Genet. Metab. *104*, 677–681.
26. Hildebrandt, F., Benzing, T., and Katsanis, N. (2011). Ciliopathies. N. Engl. J. Med. *364*, 1533–1543.
27. Braun, D.A., and Hildebrandt, F. (2017). Ciliopathies. Cold Spring Harb. Perspect. Biol. *9*, a028191.
28. Reiter, J.F., and Leroux, M.R. (2017). Genes and molecular pathways underpinning ciliopathies. Nat. Rev. Mol. Cell Biol. *18*, 533–547.
29. Wheway, G., Mitchison, H.M.; and Genomics England Research Consortium (2019). Opportunities and Challenges for Molecular Understanding of Ciliopathies-The 100,000 Genomes Project. Front. Genet. *10*, 127.
30. Nachury, M.V. (2018). The molecular machines that traffic signaling receptors into and out of cilia. Curr. Opin. Cell Biol. *51*, 124–131.
31. Jordan, M.A., and Pigino, G. (2021). The structural basis of intraflagellar transport at a glance. J. Cell Sci. *134*, jcs247163.
32. Walker, R.V., Keynton, J.L., Grimes, D.T., Sreekumar, V., Williams, D.J., Esapa, C., Wu, D., Knight, M.M., and Norris, D.P. (2019). Ciliary exclusion of Polycystin-2 promotes kidney cystogenesis in an autosomal dominant polycystic kidney disease model. Nat. Commun. *10*, 4072.
33. Garcia-Gonzalo, F.R., Corbit, K.C., Sirerol-Piquer, M.S., Ramaswami, G., Otto, E.A., Noriega, T.R., Seol, A.D., Robinson, J.F., Bennett, C.L., Josifova, D.J., et al. (2011). A transition zone complex regulates mammalian ciliogenesis and ciliary membrane composition. Nat. Genet. *43*, 776–784.
34. Legue, E., and Liem, K.F., Jr. (2019). Tulp3 Is a Ciliary Trafficking Gene that Regulates Polycystic Kidney Disease. Curr. Biol. *29*, 803–812.e5.
35. Ma, M., Tian, X., Igarashi, P., Pazour, G.J., and Somlo, S. (2013). Loss of cilia suppresses cyst growth in genetic models of autosomal dominant polycystic kidney disease. Nat. Genet. *45*, 1004–1012.
36. Schrier, R.W., Abebe, K.Z., Perrone, R.D., Torres, V.E., Braun, W.E., Steinman, T.I., Winklhofer, F.T., Brosnahan, G., Czarnecki, P.G., Hogan, M.C., et al. (2014). Blood pressure in early autosomal dominant polycystic kidney disease. N. Engl. J. Med. *371*, 2255–2266.
37. Torres, V.E., Abebe, K.Z., Chapman, A.B., Schrier, R.W., Braun, W.E., Steinman, T.I., Winklhofer, F.T., Brosnahan, G., Czarnecki, P.G., Hogan, M.C., et al. (2014). Angiotensin blockade in late autosomal dominant polycystic kidney disease. N. Engl. J. Med. *371*, 2267–2276.
38. Perrone, R.D., Abebe, K.Z., Watnick, T.J., Althouse, A.D., Hallows, K.R., Lalama, C.M., Miskulin, D.C., Seliger, S.L., Tao, C., Harris, P.C., and Bae, K.T. (2021). Primary results of the randomized trial of metformin administration in polycystic kidney disease (TAME PKD). Kidney Int. *100*, 684–696.
39. Meijer, E., Visser, F.W., van Aerts, R.M.M., Blijdorp, C.J., Casteleijn, N.F., D'Agnolo, H.M.A., Dekker, S.E.I., Drenth, J.P.H., de Fijter, J.W., van Gastel, M.D.A., et al. (2018). Effect of Lanreotide on Kidney Function in Patients With Autosomal Dominant Polycystic Kidney Disease: The DIPAK 1 Randomized Clinical Trial. JAMA *320*, 2010–2019.
40. Grantham, J.J., Torres, V.E., Chapman, A.B., Guay-Woodford, L.M., Bae, K.T., King, B.F., Jr., Wetzel, L.H., Baumgarten, D.A., Kenney, P.J., Harris, P.C., et al. (2006). Volume progression in polycystic kidney disease. N. Engl. J. Med. *354*, 2122–2130.
41. Cornec-Le Gall, E., Audrézet, M.P., Rousseau, A., Hourmant, M., Renaudineau, E., Charasse, C., Morin, M.P., Moal, M.C., Dantal, J., Wehbe, B., et al. (2016). The PROPKD Score: A New Algorithm to Predict Renal Survival in Autosomal Dominant Polycystic Kidney Disease. J. Am. Soc. Nephrol. *27*, 942–951.
42. Messchendorp, A.L., Meijer, E., Visser, F.W., Engels, G.E., Kappert, P., Losekoot, M., Peters, D.J.M., Gansevoort, R.T.; and on behalf of the DIPAK-1 study investigators (2019). Rapid Progression of Autosomal Dominant Polycystic Kidney Disease: Urinary Biomarkers as Predictors. Am. J. Nephrol. *50*, 375–385.
43. Benson, K.A., Murray, S.L., Senum, S.R., Elhassan, E., Conlon, E.T., Kennedy, C., Conlon, S., Gilbert, E., Connaughton, D., O'Hara, P., et al. (2021). The genetic landscape of polycystic kidney disease in Ireland. Eur. J. Hum. Genet. *29*, 827–838.
44. Kline, T.L., Korfiatis, P., Edwards, M.E., Warner, J.D., Irazabal, M.V., King, B.F., Torres, V.E., and Erickson, B.J. (2016). Automatic total kidney volume measurement on follow-up magnetic resonance images to facilitate monitoring of autosomal dominant polycystic kidney disease progression. Nephrol. Dial. Transplant. *31*, 241–248.
45. Levey, A.S., Stevens, L.A., Schmid, C.H., Zhang, Y.L., Castro, A.F., 3rd, Feldman, H.I., Kusek, J.W., Eggers, P., Van Lente, F., Greene, T., Coresh, J.; and CKD-EPI (Chronic Kidney Disease Epidemiology Collaboration) (2009). A new equation to estimate glomerular filtration rate. Ann. Intern. Med. *150*, 604–612.
46. Hopp, K., Cornec-Le Gall, E., Senum, S.R., Te Paske, I.B.A.W., Raj, S., Lavu, S., Baheti, S., Edwards, M.E., Madsen, C.D., Heyer, C.M., et al. (2020). Detection and characterization of mosaicism in autosomal dominant polycystic kidney disease. Kidney Int. *97*, 370–382.
47. Richards, S., Aziz, N., Bale, S., Bick, D., Das, S., Gastier-Foster, J., Grody, W.W., Hegde, M., Lyon, E., Spector, E., et al. (2015). Standards and guidelines for the interpretation of sequence variants: a joint consensus recommendation of the American College of Medical Genetics and Genomics and the Association for Molecular Pathology. Genet. Med. *17*, 405–424.

48. Reese, M.G., Eeckman, F.H., Kulp, D., and Haussler, D. (1997). Improved splice site detection in Genie. J. Comput. Biol. *4*, 311–323.
49. Desmet, F.O., Hamroun, D., Lalande, M., Collod-Béroud, G., Claustres, M., and Béroud, C. (2009). Human Splicing Finder: an online bioinformatics tool to predict splicing signals. Nucleic Acids Res. *37*, e67.
50. Sudlow, C., Gallacher, J., Allen, N., Beral, V., Burton, P., Danesh, J., Downey, P., Elliott, P., Green, J., Landray, M., et al. (2015). UK biobank: an open access resource for identifying the causes of a wide range of complex diseases of middle and old age. PLoS Med. *12*, e1001779.
51. Van Hout, C.V., Tachmazidou, I., Backman, J.D., Hoffman, J.D., Liu, D., Pandey, A.K., Gonzaga-Jauregui, C., Khalid, S., Ye, B., Banerjee, N., et al. (2020). Exome sequencing and characterization of 49,960 individuals in the UK Biobank. Nature *586*, 749–756.
52. Wang, Q., Dhindsa, R.S., Carss, K., Harper, A.R., Nag, A., Tachmazidou, I., Vitsios, D., Deevi, S.V.V., Mackay, A., Muthas, D., et al. (2021). Rare variant contribution to human disease in 281,104 UK Biobank exomes. Nature *597*, 527–532.
53. Pei, Y., Obaji, J., Dupuis, A., Paterson, A.D., Magistroni, R., Dicks, E., Parfrey, P., Cramer, B., Coto, E., Torra, R., et al. (2009). Unified criteria for ultrasonographic diagnosis of ADPKD. J. Am. Soc. Nephrol. *20*, 205–212.
54. Pei, Y., Hwang, Y.H., Conklin, J., Sundsbak, J.L., Heyer, C.M., Chan, W., Wang, K., He, N., Rattansingh, A., Atri, M., et al. (2015). Imaging-based diagnosis of autosomal dominant polycystic kidney disease. J. Am. Soc. Nephrol. *26*, 746–753.
55. Hirano, T., Katoh, Y., and Nakayama, K. (2017). Intraflagellar transport-A complex mediates ciliary entry and retrograde trafficking of ciliary G protein-coupled receptors. Mol. Biol. Cell *28*, 429–439.
56. Scheidel, N., and Blacque, O.E. (2018). Intraflagellar Transport Complex A Genes Differentially Regulate Cilium Formation and Transition Zone Gating. Curr. Biol. *28*, 3279–3287.e2.
57. Picariello, T., Brown, J.M., Hou, Y., Swank, G., Cochran, D.A., King, O.D., Lechtreck, K., Pazour, G.J., and Witman, G.B. (2019). A global analysis of IFT-A function reveals specialization for transport of membrane-associated proteins into cilia. J. Cell Sci. *132*, jcs220749.
58. Perrault, I., Saunier, S., Hanein, S., Filhol, E., Bizet, A.A., Collins, F., Salih, M.A., Gerber, S., Delphin, N., Bigot, K., et al. (2012). Mainzer-Saldino syndrome is a ciliopathy caused by IFT140 mutations. Am. J. Hum. Genet. *90*, 864–870.
59. Schmidts, M., Frank, V., Eisenberger, T., Al Turki, S., Bizet, A.A., Antony, D., Rix, S., Decker, C., Bachmann, N., Bald, M., et al. (2013). Combined NGS approaches identify mutations in the intraflagellar transport gene IFT140 in skeletal ciliopathies with early progressive kidney Disease. Hum. Mutat. *34*, 714–724.
60. Bayat, A., Kerr, B., Douzgou, S.; and DDD Study (2017). The evolving craniofacial phenotype of a patient with Sensenbrenner syndrome caused by IFT140 compound heterozygous mutations. Clin. Dysmorphol. *26*, 247–251.
61. Hull, S., Owen, N., Islam, F., Tracey-White, D., Plagnol, V., Holder, G.E., Michaelides, M., Carss, K., Raymond, F.L., Rozet, J.M., et al. (2016). Nonsyndromic Retinal Dystrophy due to Bi-Allelic Mutations in the Ciliary Transport Gene IFT140. Invest. Ophthalmol. Vis. Sci. *57*, 1053–1062.
62. Xu, M., Yang, L., Wang, F., Li, H., Wang, X., Wang, W., Ge, Z., Wang, K., Zhao, L., Li, H., et al. (2015). Mutations in human IFT140 cause non-syndromic retinal degeneration. Hum. Genet. *134*, 1069–1078.
63. Jonassen, J.A., SanAgustin, J., Baker, S.P., and Pazour, G.J. (2012). Disruption of IFT complex A causes cystic kidneys without mitotic spindle misorientation. J. Am. Soc. Nephrol. *23*, 641–651.
64. Taliun, D., Harris, D.N., Kessler, M.D., Carlson, J., Szpiech, Z.A., Torres, R., Taliun, S.A.G., Corvelo, A., Gogarten, S.M., Kang, H.M., et al. (2021). Sequencing of 53,831 diverse genomes from the NHLBI TOPMed Program. Nature *590*, 290–299.
65. Pottel, H., Hoste, L., Dubourg, L., Ebert, N., Schaeffner, E., Eriksen, B.O., Melsom, T., Lamb, E.J., Rule, A.D., Turner, S.T., et al. (2016). An estimated glomerular filtration rate equation for the full age spectrum. Nephrol. Dial. Transplant. *31*, 798–806.
66. Seliger, S.L., Watnick, T., Althouse, A.D., Perrone, R.D., Abebe, K.Z., Hallows, K.R., Miskulin, D.C., and Bae, K.T. (2020). Baseline Characteristics and Patient-Reported Outcomes of ADPKD Patients in the Multicenter TAME-PKD Clinical Trial. Kidney360 *1*, 1363–1372.
67. Schrier, R.W., Johnson, A.M., McFann, K., and Chapman, A.B. (2003). The role of parental hypertension in the frequency and age of diagnosis of hypertension in offspring with autosomal-dominant polycystic kidney disease. Kidney Int. *64*, 1792–1799.
68. Reed, B., McFann, K., Kimberling, W.J., Pei, Y., Gabow, P.A., Christopher, K., Petersen, E., Kelleher, C., Fain, P.R., Johnson, A., and Schrier, R.W. (2008). Presence of de novo mutations in autosomal dominant polycystic kidney disease patients without family history. Am. J. Kidney Dis. *52*, 1042–1050.
69. Waanders, E., te Morsche, R.H., de Man, R.A., Jansen, J.B., and Drenth, J.P. (2006). Extensive mutational analysis of PRKCSH and SEC63 broadens the spectrum of polycystic liver disease. Hum. Mutat. *27*, 830.
70. Besse, W., Choi, J., Ahram, D., Mane, S., Sanna-Cherchi, S., Torres, V., and Somlo, S. (2018). A noncoding variant in GANAB explains isolated polycystic liver disease (PCLD) in a large family. Hum. Mutat. *39*, 378–382.
71. Wilson, G.J., Wood, S., Patel, C., Oliver, K., John, G., Ranganathan, D., Mallett, A., and Isbel, N. (2020). *DNAJB11*-Related Atypical ADPKD in a Kidney Transplant Donor. Kidney Int. Rep. *5*, 1363–1366.
72. Delbarba, E., Econimo, L., Dordoni, C., Martin, E., Mazza, C., Savoldi, G., Alberici, F., Scolari, F., and Izzi, C. (2021). Expanding the variability of the ADPKD-GANAB clinical phenotype in a family of Italian ancestry. J. Nephrol. https://doi.org/10.1007/s40620-40021-01131-w.
73. Mallawaarachchi, A.C., Lundie, B., Hort, Y., Schonrock, N., Senum, S.R., Gayevskiy, V., Minoche, A.E., Hollway, G., Ohnesorg, T., Hinchcliffe, M., et al. (2021). Genomic diagnostics in polycystic kidney disease: an assessment of real-world use of whole-genome sequencing. Eur. J. Hum. Genet. *29*, 760–770.
74. Pei, Y., Paterson, A.D., Wang, K.R., He, N., Hefferton, D., Watnick, T., Germino, G.G., Parfrey, P., Somlo, S., and St George-Hyslop, P. (2001). Bilineal disease and trans-heterozygotes in autosomal dominant polycystic kidney disease. Am. J. Hum. Genet. *68*, 355–363.
75. Bergmann, C., von Bothmer, J., Ortiz Brüchle, N., Venghaus, A., Frank, V., Fehrenbach, H., Hampel, T., Pape, L., Buske, A., Jonsson, J., et al. (2011). Mutations in multiple PKD genes

may explain early and severe polycystic kidney disease. J. Am. Soc. Nephrol. *22*, 2047–2056.
76. Fedeles, S.V., Tian, X., Gallagher, A.R., Mitobe, M., Nishio, S., Lee, S.H., Cai, Y., Geng, L., Crews, C.M., and Somlo, S. (2011). A genetic interaction network of five genes for human polycystic kidney and liver diseases defines polycystin-1 as the central determinant of cyst formation. Nat. Genet. *43*, 639–647.
77. Gainullin, V.G., Hopp, K., Ward, C.J., Hommerding, C.J., and Harris, P.C. (2015). Polycystin-1 maturation requires polycystin-2 in a dose-dependent manner. J. Clin. Invest. *125*, 607–620.
78. Olson, R.J., Hopp, K., Wells, H., Smith, J.M., Furtado, J., Constans, M.M., Escobar, D.L., Geurts, A.M., Torres, V.E., and Harris, P.C. (2019). Synergistic Genetic Interactions between *Pkhd1* and *Pkd1* Result in an ARPKD-Like Phenotype in Murine Models. J. Am. Soc. Nephrol. *30*, 2113–2127.
79. Vujic, M., Heyer, C.M., Ars, E., Hopp, K., Markoff, A., Orndal, C., Rudenhed, B., Nasr, S.H., Torres, V.E., Torra, R., et al. (2010). Incompletely penetrant *PKD1* alleles mimic the renal manifestations of ARPKD. J. Am. Soc. Nephrol. *21*, 1097–1102.
80. Audrézet, M.P., Corbiere, C., Lebbah, S., Morinière, V., Broux, F., Louillet, F., Fischbach, M., Zaloszyc, A., Cloarec, S., Merieau, E., et al. (2016). Comprehensive PKD1 and PKD2 Mutation Analysis in Prenatal Autosomal Dominant Polycystic Kidney Disease. J. Am. Soc. Nephrol. *27*, 722–729.
81. Losekoot, M., Ruivenkamp, C.A., Tholens, A.P., Grimbergen, J.E., Vijfhuizen, L., Vermeer, S., Dijkman, H.B., Cornelissen, E.A., Bongers, E.M., and Peters, D.J. (2012). Neonatal onset autosomal dominant polycystic kidney disease (ADPKD) in a patient homozygous for a PKD2 missense mutation due to uniparental disomy. J. Med. Genet. *49*, 37–40.
82. Jordan, P., Arrondel, C., Bessières, B., Tessier, A., Attié-Bitach, T., Guterman, S., Morinière, V., Antignac, C., Saunier, S., Gubler, M.C., and Heidet, L. (2021). Bi-allelic pathogenic variations in DNAJB11 cause Ivemark II syndrome, a renal-hepatic-pancreatic dysplasia. Kidney Int. *99*, 405–409.
83. Ateş, E.A., Turkyilmaz, A., Delil, K., Alavanda, C., Söylemez, M.A., Geçkinli, B.B., Ata, P., and Arman, A. (2021). Biallelic Mutations in *DNAJB11* are Associated with Prenatal Polycystic Kidney Disease in a Turkish Family. Mol. Syndromol. *12*, 179–185.
84. Frank, C.G., Grubenmann, C.E., Eyaid, W., Berger, E.G., Aebi, M., and Hennet, T. (2004). Identification and functional analysis of a defect in the human ALG9 gene: definition of congenital disorder of glycosylation type IL. Am. J. Hum. Genet. *75*, 146–150.
85. Chantret, I., Dancourt, J., Dupré, T., Delenda, C., Bucher, S., Vuillaumier-Barrot, S., Ogier de Baulny, H., Peletan, C., Danos, O., Seta, N., et al. (2003). A deficiency in dolichyl-P-glucose:Glc1Man9GlcNAc2-PP-dolichyl alpha3-glucosyltransferase defines a new subtype of congenital disorders of glycosylation. J. Biol. Chem. *278*, 9962–9971.
86. Lu, W., Peissel, B., Babakhanlou, H., Pavlova, A., Geng, L., Fan, X., Larson, C., Brent, G., and Zhou, J. (1997). Perinatal lethality with kidney and pancreas defects in mice with a targetted Pkd1 mutation. Nat. Genet. *17*, 179–181.
87. Bergmann, C., Senderek, J., Sedlacek, B., Pegiazoglou, I., Puglia, P., Eggermann, T., Rudnik-Schöneborn, S., Furu, L., Onuchic, L.F., De Baca, M., et al. (2003). Spectrum of mutations in the gene for autosomal recessive polycystic kidney disease (ARPKD/PKHD1). J. Am. Soc. Nephrol. *14*, 76–89.
88. Hopp, K., Ward, C.J., Hommerding, C.J., Nasr, S.H., Tuan, H.F., Gainullin, V.G., Rossetti, S., Torres, V.E., and Harris, P.C. (2012). Functional polycystin-1 dosage governs autosomal dominant polycystic kidney disease severity. J. Clin. Invest. *122*, 4257–4273.
89. Qian, F., Watnick, T.J., Onuchic, L.F., and Germino, G.G. (1996). The molecular basis of focal cyst formation in human autosomal dominant polycystic kidney disease type I. Cell *87*, 979–987.
90. Piontek, K., Menezes, L.F., Garcia-Gonzalez, M.A., Huso, D.L., and Germino, G.G. (2007). A critical developmental switch defines the kinetics of kidney cyst formation after loss of Pkd1. Nat. Med. *13*, 1490–1495.
91. Tan, A.Y., Zhang, T., Michaeel, A., Blumenfeld, J., Liu, G., Zhang, W., Zhang, Z., Zhu, Y., Rennert, L., Martin, C., et al. (2018). Somatic Mutations in Renal Cyst Epithelium in Autosomal Dominant Polycystic Kidney Disease. J. Am. Soc. Nephrol. *29*, 2139–2156.
92. Lantinga-van Leeuwen, I.S., Dauwerse, J.G., Baelde, H.J., Leonhard, W.N., van de Wal, A., Ward, C.J., Verbeek, S., Deruiter, M.C., Breuning, M.H., de Heer, E., and Peters, D.J. (2004). Lowering of Pkd1 expression is sufficient to cause polycystic kidney disease. Hum. Mol. Genet. *13*, 3069–3077.
93. Rossetti, S., Kubly, V.J., Consugar, M.B., Hopp, K., Roy, S., Horsley, S.W., Chauveau, D., Rees, L., Barratt, T.M., van't Hoff, W.G., et al. (2009). Incompletely penetrant PKD1 alleles suggest a role for gene dosage in cyst initiation in polycystic kidney disease. Kidney Int. *75*, 848–855.
94. Durkie, M., Chong, J., Valluru, M.K., Harris, P.C., and Ong, A.C.M. (2021). Biallelic inheritance of hypomorphic PKD1 variants is highly prevalent in very early onset polycystic kidney disease. Genet. Med. *23*, 689–697.
95. Brasier, J.L., and Henske, E.P. (1997). Loss of the polycystic kidney disease (*PKD1*) region of chromosome 16p13 in renal cyst cells supports a loss-of-function model for cyst pathogenesis. J. Clin. Invest. *99*, 194–199.
96. Brook-Carter, P.T., Peral, B., Ward, C.J., Thompson, P., Hughes, J., Maheshwar, M.M., Nellist, M., Gamble, V., Harris, P.C., and Sampson, J.R. (1994). Deletion of the *TSC2* and *PKD1* genes associated with severe infantile polycystic kidney disease–a contiguous gene syndrome. Nat. Genet. *8*, 328–332.
97. Sampson, J.R., Maheshwar, M.M., Aspinwall, R., Thompson, P., Cheadle, J.P., Ravine, D., Roy, S., Haan, E., Bernstein, J., and Harris, P.C. (1997). Renal cystic disease in tuberous sclerosis: role of the polycystic kidney disease 1 gene. Am. J. Hum. Genet. *61*, 843–851.